Brain Structure and Function (2018) 223:3689–3709
https://doi.org/10.1007/s00429-018-1715-0

ORIGINAL ARTICLE

Cell type-specific effects of BDNF in modulating dendritic architecture of hippocampal neurons

Marta Zagrebelsky[1] · N. Gödecke[1] · A. Remus[1,2] · Martin Korte[1,2]

Received: 16 January 2018 / Accepted: 9 July 2018 / Published online: 18 July 2018

Abstract

Brain-derived neurotrophin factor (BDNF) has been implicated in neuronal survival, differentiation and activity-dependent synaptic plasticity in the central nervous system. It was suggested that during postnatal development BDNF regulates neuronal architecture and spine morphology of neurons within certain brain areas but not others. Particularly striking are the differences between striatum, cortex and hippocampus. Whether this is due to region- or cell type-specific effects is so far not known. We address this question using conditional *bdnf* knock-out mice to analyze neuronal architecture and spine morphology of pyramidal cortical and hippocampal neurons as well as inhibitory neurons from these brain areas and excitatory granule neurons from the dentate gyrus. While hippocampal and cortical inhibitory neurons and granule cells of the dentate gyrus are strongly impaired in their architecture, pyramidal neurons within the same brain regions only show a mild phenotype. We found a reduced TrkB phosphorylation within hippocampal interneurons and granule cells of the dentate gyrus, accompanied by a significant decrease in dendritic complexity. In contrast, in pyramidal neurons both TrkB phosphorylation and neuronal architecture are not altered. The results suggest diverse levels of responsiveness to BDNF for different hippocampal and cortical neuronal populations within the same brain area. Among the possible mechanisms mediating these differences in BDNF function, we tested whether zinc might be involved in TrkB transactivation specifically in pyramidal neurons. We propose that a BDNF-independent transactivation of TrkB receptor may be able to compensate the lack of BDNF signaling to modulate neuronal morphology in a cell type-specific manner.

Keywords Dendrites · Spines · Structural plasticity · Hippocampus · TrkB · Zinc

Introduction

Brain-derived neurotrophin factor (BDNF) has been proposed to be a crucial factor in promoting neuronal survival, differentiation and activity-dependent synaptic plasticity in the central nervous system (CNS). A role of BDNF in regulating neuronal architecture and spine morphology in an activity-dependent manner has been especially shown in vitro by its exogenous application to cortical and hippocampal neurons (McAllister et al. 1995, 1996; Horch et al. 1999; Tyler and Pozzo-Miller 2001, 2003; Ji et al. 2005, 2010; Kwon and Sabatini 2011; Kellner et al. 2014). In vivo the physiological variability in BDNF expression levels in the mouse dentate gyrus is correlated to the dendritic spine density in granule cells (Stranahan 2011) and a reduction of serum levels of BDNF is associated to a reduction in hippocampal volume in aging humans (Erickson et al. 2010) as well as in dendritic complexity and spine density in senescent rats (von Bohlen und Halbach 2010). However, the

Marta Zagrebelsky and N. Gödecke contributed equally to this work.

Electronic supplementary material The online version of this article (https://doi.org/10.1007/s00429-018-1715-0) contains supplementary material, which is available to authorized users.

✉ Marta Zagrebelsky
m.zagrebelsky@tu-bs.de

✉ Martin Korte
m.korte@tu-bs.de

[1] Division of Cellular Neurobiology, Zoological Institute, TU Braunschweig, Spielmannstr. 7, 38106 Brunswick, Germany

[2] Helmholtz Centre for Infection Research, AG NIND, Inhoffenstr. 7, 38124 Brunswick, Germany

in vivo role of BDNF has been very difficult to confirm in the postnatal brain as *bdnf* conventional knockouts die early after birth (Jones et al. 1994) before the increase in BDNF expression during the first three postnatal weeks (Castren et al. 1992) and the structural maturation of the neuronal circuitry. Thus, a number of studies have been performed using different conditional gene targeted mouse lines and Cre-loxP-mediated excision of *bdnf* (Rios et al. 2001; Gorski et al. 2003; Baquet et al. 2004; He et al. 2004a; Chan et al. 2006, 2008; Monteggia et al. 2007; Unger et al. 2007; Rauskolb et al. 2010). Surprisingly, analyzing the effect on the architecture of neurons of a global BDNF deprivation throughout the CNS revealed an astonishing selectivity in the brain areas requiring BDNF for their postnatal development. Rauskolb et al. (2010) showed that in a Tau-*bdnf* ko mouse the volume of the cortex is only slightly reduced and the one of the hippocampus is unchanged. Accordingly, dendritic complexity of CA1 pyramidal cells is only mildly reduced and while no changes could be observed in dendritic spine density the spine type distribution is significantly shifted toward a more immature phenotype, pointing to a specific role of BDNF in the maintenance of dendritic spines in the hippocampus. On the other hand, the volume of the striatum in Tau-*bdnf* ko mice is strongly reduced and striatal neurons show a significant reduction in dendritic length and complexity as well as a dramatic decrease in dendritic spine density (Rauskolb et al. 2010). The results obtained from Rauskolb et al. (2010) indicate a fundamental difference in the role of BDNF in regulating the dendritic architecture of striatal versus hippocampal neurons. Whether this is due to an area-specific effect or rather a cell type-specific effect of BDNF remains an open question and is addressed in our current study. Moreover, the molecular mechanisms mediating the different sensitivity of neurons to BDNF are still largely unexplored. The effects of BDNF in regulating neuronal architecture and dendritic spine maturation have been shown to be mediated by its binding to and activating of the TrkB receptor (Tyler and Pozzo-Miller 2001, 2003; Ji et al. 2010; Kellner et al. 2014; Zagrebelsky and Korte 2014). BDNF is indeed, considered to be the prototypical neurotrophin ligand for the TrkB receptor. However, the divalent cation zinc has been shown to transactivate TrkB in a BDNF-independent, Src family kinase-dependent manner and thus resulting in the potentiation of the mossy fiber-CA3 synapses (Huang et al. 2008). Interestingly, zinc is present at glutamatergic synapses throughout the cortex and hippocampus (Frederickson and Danscher 1990; Choi and Koh 1998; Frederickson et al. 2005) and is co-released with glutamate in an activity-dependent manner. The results presented here support the possibility that zinc-mediated TrkB transactivation may be involved in controlling the neuronal architecture in cortical and hippocampal pyramidal neurons upon a global BDNF deletion.

Materials and methods

Mice

The conditional *bdnf* knock-out mouse (c*bdnf ko*) was generated in the group of Yves-Alain Barde by using the Cre-loxP recombination system (Rauskolb et al. 2010). Briefly, mice carrying two floxed *bdnf* alleles ($bdnf^{lox/lox}$) were crossed with a mouse line expressing a Cre-recombinase on one allele of the tau locus tau::cre line (Korets-Smith et al. 2004); and which additionally carries one floxed *bdnf* allele. Genotypes of the animals were determined by PCR as previously described (Rauskolb et al. 2010) using a tail biopsy. Mice were housed under standard laboratory conditions with controlled temperature (20–22 °C), a 12 h light–dark cycle and with ad libitum access to food and water. All animals used in this study were kept on a C57BL/6J-SV129 genetic background and littermate mice with the following genotype $bdnf^{lox/lox}$ or $bdnf^{wt}$ used as controls. All experiments were carried out at the age of 8 weeks. All procedures concerning animals were approved by the animal welfare representative of the TU Braunschweig and the LAVES (Oldenburg, Germany, Az. §4 (02.05) TSchB TU BS).

Cell culture and treatments

Primary cultures of mouse hippocampal, cortical and striatal neurons were prepared from mice carrying two floxed *bdnf* alleles at embryonic day E16.5. Embryos were rapidly decapitated and the brains were kept in ice-cold Gey's balanced salt solution (GBSS) containing 50% glucose and adjusted to pH 7.3. The hippocampi, striata and cortices were dissected, the different brain regions were incubated for 30 min in trypsin/EDTA at 37 °C and then mechanically dissociated. Cells were plated at a density of 70×10^4 cells/cm^2 on poly-L-lysine-coated coverslips (12 mm) and kept in neurobasal medium supplemented with 200 mM glutamine, 1% N_2 supplement, 2% B27 supplement. For mixed cortico-striatal cultures the cells suspension from the striatum and from the cortex were mixed in 1:1 ratio before plating. 3 h after preparation the primary cultures were transduced with a CMV-driven Cre-recombinase/eGFP expressing lentivirus. The expression of the Cre-recombinase was visualized by the co-expression of eGFP starting 7 days after transduction. Transduced hippocampal neurons were incubated for 3 weeks at 37 °C and 5% CO_2 and 99% humidity. In a set of experiments hippocampal primary neurons were treated with 0.5 µg/ml TrkB-Fc receptor bodies (R&D Systems) every second day, starting at 2 days in vitro (DIV 2) up to DIV20

or with 40 ng/ml recombinant BDNF (R&D Systems) at DIV2, 4, 6 12 and 16. In another set of experiments, the hippocampal neurons were treated with 1.5 mM CaEDTA (Sigma-Aldrich) during the first week in culture and repeatedly treated with or without 50 µM $ZnCl_2$ or 0.5 µM SKF-inhibitor PP1 (Sigma-Aldrich; Huang et al. 2008; Frederickson et al. 2002) every 7 days starting at DIV 1 up to DIV 20. The health of the neurons was assessed looking at their morphology upon transfection with mCherry. Only neurons not showing any sign of degeneration (dendrite fragmentation, retraction bulbs and a hairy soma) were imaged and included in the analysis.

Transfection and immunohistochemistry

At 20 DIV, cultured neurons were transfected with 0.8 µg of the DNA expression plasmid for mCherry under a CMV promoter using Lipofectamine® 2000 transfection reagent (ThermoFisher Scientific) according to the manufactures' instructions. 24 h after the transfection, primary hippocampal cultures were fixed in 4% PFA in 0.2 M PB at 4 °C for 15 min followed by a blocking and permeabilization step performed at room temperature in PBS containing 1% bovine serum albumin, 10% goat serum and 0.2% Triton X-100 for 1 h. All primary antibodies were diluted in PBS containing 10% goat serum and incubated overnight at 4 °C. The following primary antibodies were used: against BDNF (1:1000, Yves Barde), phospho-TrkA (Tyr674/675)/TrkB (Tyr706/707) (1:500, Cell Signaling Technology), Prox-1 (1:500; Millipore), CamKinaseII (1:500, Life technologies), Ctip2 (1:500, Abcam) calbindin (1:7000, Swant), calretinin (1:5000, Swant) and parvalbumin (1:5000, Swant). Appropriate secondary antibodies and conjugated fluorochromes were selected for double immunofluorescence analysis. After washing the cultures were counterstained using 4′,6-diamidino-2-phenylindole (DAPI) to label cell nuclei and mounted in aqueous medium containing anti-fading agents (Biomeda, CA, USA). In one set of experiments DIV 8 cultured neurons were transfected with 0.5 µg each of DNA expression plasmid for mCherry and for specific shRNAs for the zinc transporter ZnT-3 (Santa Cruz Biotechnology). At DIV21 the neurons were fixed in 4% PFA and the downregulation of ZnT-3 was assessed by immunohistochemistry using a monoclonal antibody against ZnT-3 (1:100, Synaptic Systems).

BDNF immunoassay

In order to quantify the amount of BDNF within the supernatant of primary hippocampal cultures, BDNF sandwich ELISA (BEK-2003-2P, Biosensis) was performed according to the manufactures' instructions. Recombinant mouse BDNF was used as standard (7.8–1000 pg/ml recombinant BDNF). Briefly, 100 µl/well of BDNF standard and the respective samples were applied to the pre-coated microtiter plate and incubated overnight at 4 °C gently shacking. The plate was then washed with 0.01 M PBS, incubated with a biotinylated BDNF antibody for 2 h at room temperature (RT) and incubated with an avidin–biotin–peroxidase complex for 1 h at RT. Finally, TMB (3,3′,5,5′-tetramethylbenzidine) solution was added to the plate and after 15 min the reaction was stopped with a TMP stop solution. Extinction of the color reaction was measured immediately at a wavelength of 450 nm using a microplate reader (Dynatech Laboratories). The BDNF concentration within the cell culture supernatant was interpolated from the BDNF standard curve using linear regression analysis. Statistical analyses were performed with Microsoft Excel and GraphPad Prism. Data obtained were tested for significance using either with a two-tailed unpaired Student's *t* test for the comparison of two independent means, or with a one-way ANOVA and Tukey's post hoc test for multiple comparison. All data are presented as mean ± SEM. Significance levels are indicated as $*p < 0.05$; $**p < 0.01$; $***p < 0.001$.

BDNF depletion in primary hippocampal cultures

To verify the extent of depletion for the BDNF protein, immunoreactivity for BDNF was compared for 21 DIV hippocampal primary cultures derived from BDNF floxed mice either transduced (BDNFΔ) or not transduced (control) with lentiviruses to express the Cre-recombinase as well as eGFP (Ubc CRIG). In control cultures eGFP was completely absent and BDNF immunohistochemistry showed a strong diffuse signal within most of the neurons (Fig. 1j, above). In 21 DIV cultures, transduced with Ubc CRIG most hippocampal neurons were positive for eGFP and completely lacked the BDNF immunoreactivity (Fig. 1j, below). Moreover, the changes over time in BDNF concentration within the supernatant of control and Ubc CRIG transduced hippocampal primary cultures were analyzed using ELISA. While, as expected the BDNF concentration in the supernatant of control cultures (grey) progressively increased during the 3 weeks of cultivation, upon Ubc CRIG transduction BDNF (red) concentrations slightly decreased over time being significantly lower than under control conditions by DIV 21 ($p < 0.05$; Fig. 1k; DIV7: 16 ± 7.48 vs. 24 ± 5.81, DIV14: 29 ± 7.66 vs. 15 ± 3.86, DIV21 41 ± 7.45 vs. 11 ± 2.80).

Brain slice preparation and DiOlistic

DiOlistic technique was performed as previously described (Rauskolb et al. 2010). Briefly, 8-week-old wild type and *cbdnf ko* mice were transcardially perfused with 0.1 M phosphate buffer (PB) pH 7.4, containing 4% PFA and 4% sucrose. The brains were dissected, kept for 30 min in 4% PFA in 0.1 M PB for post-fixation at 4 °C, embedded in

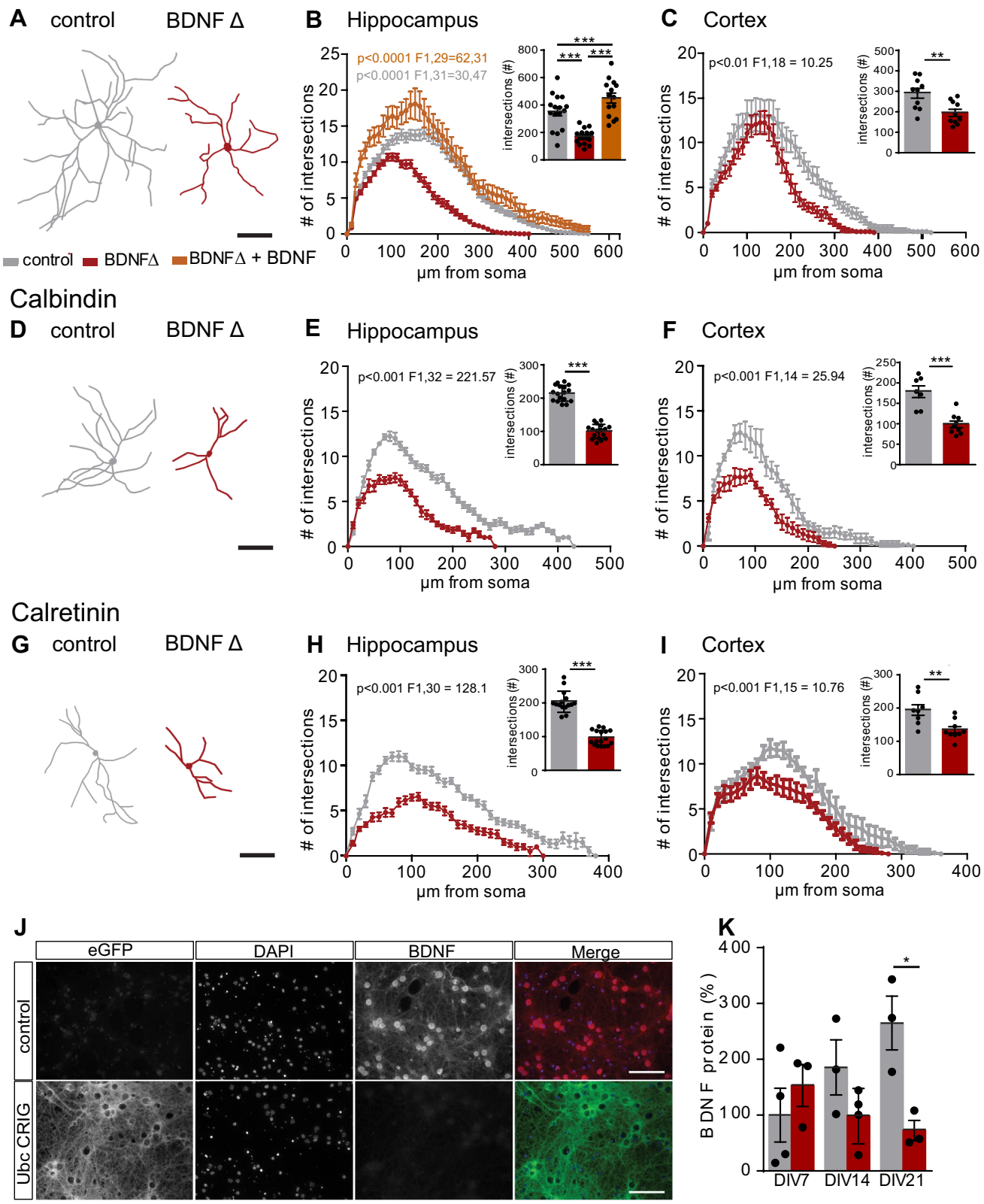
Parvalbumin
A control
BDNF Δ
B Hippocampus
C Cortex
p<0.0001 F1,29=62,31
p<0.0001 F1,31=30,47
p<0.01 F1,18 = 10.25
# of intersections
μm from soma
intersections (#)
control
BDNFΔ
BDNFΔ + BDNF
Calbindin
D control
BDNF Δ
E Hippocampus
F Cortex
p<0.001 F1,32 = 221.57
p<0.001 F1,14 = 25.94
Calretinin
G control
BDNF Δ
H Hippocampus
I Cortex
p<0.001 F1,30 = 128.1
p<0.001 F1,15 = 10.76
J
eGFP
DAPI
BDNF
Merge
control
Ubc CRIG
K
BDNF protein (%)
DIV7
DIV14
DIV21

◂**Fig. 1** Dendritic morphology of cortical and hippocampal inhibitory neurons from control and BDNF-depleted primary cultures. Representative tracings, respectively, showing the neuronal morphology of parvalbumin- (**a**), calbindin- (**d**) and calretinin-positive (**g**) control (grey) and BDNF-depleted (BDNFΔ, red) interneurons in the hippocampus. *F* values written in grey refer to the control vs. BDNFΔ comparison, those in orange refer to the BDNFΔ versus BDNFΔ + BDNF comparison. Sholl analysis showing dendritic complexity plotted against the distance from the soma and total dendritic complexity (inserts) for control and BDNF-depleted hippocampal interneurons expressing parvalbumin (**b**, $n = 16$ control, 17 BDNFΔ), calbindin (**e**, $n = 17$ control, 17 BDNFΔ) or calretinin (**h**, $n = 15$ control, 17 BDNFΔ) and for BDNF-depleted hippocampal interneurons treated with BDNF (**b**, BDNFΔ + BDNF, orange $n = 14$ BDNFΔ + BDNF). Sholl analysis showing dendritic complexity plotted against the distance from the soma and total dendritic complexity (inserts) for cortical interneurons expressing parvalbumin (**c**, $n = 10$ control, 10 BDNFΔ), calbindin (**f**, $n = 7$ control, 9 BDNFΔ) or calretinin (**i**, $n = 8$ control, 9 BDNFΔ) in hippocampal primary cultures. **j** Micrograph showing the expression of eGFP in BDNF-depleted (below) but not in control (above) hippocampal primary cultures. In control cultures most of the neurons express BDNF (red, above) while they are negative in BDNF-depleted cultures (below). Scale bar is 100 µm. **k** Graph showing the results of the ELISA measurements for BDNF in the supernatant of primary hippocampal cultures. While in control cultures BDNF (control grey, $n = 4$) progressively increases from DIV 7 to DIV21, in cultures transduced with the Ubc-CRIG virus (BDNFΔ red, $n = 3$) BDNF concentration in the supernatant progressively decreases. All data are presented as mean ± SEM. Statistical analysis was performed using an unpaired two-tailed Student's *t* test: $^{*}p < 0.05$; $^{**}p < 0.01$, $^{***}p < 0.001$

low-melting point agarose (2%) and cut transversally in 400-µm-thick slices using a vibrating microtome (VT1200S, Leica Microsystems). After cutting the brain slices were fixed in 4% PFA for 2 h at 4 °C. Hippocampal and cortical neurons were labeled with the lipophilic dye DiI (3 mg diluted in 100 µl methylene chloride) coated on tungsten particles (50 mg, M-25, 1.7 µm in diameter; Bio-Rad). DiI-coated tungsten particles were coated onto the walls of TEFZEL tubing and cut into 13-mm-long pieces. The tungsten particles were delivered to the tissue using a hand-held gene gun (Helios Gene Gun System, Bio-Rad) at a pressure of 120 psi. To prevent large particle clusters from damaging the tissue, a membrane filter (3 µm, Millipore) was inserted between the barrel aligner and the brain slice. After shooting, the brain slices were kept overnight in PBS at room temperature for the dye to diffuse. Slices were washed with PBS and post-fixed for 2 h with 4% PFA at 4 °C, counter stained with DAPI and mounted with a water-based antifading mounting medium (Biomeda).

Imaging

To analyze the dendritic architecture of DiI-labeled pyramidal neurons from the CA1 region of the Hippocampus, Layer II/III and V of the somatosensory cortex and dentate gyrus granule cells were imaged using an Axioplan 2 imaging microscope (Zeiss) equipped with an ApoTome module (Zeiss) and optical sections spaced 1 µm apart were taken from each neuron with a 20× objective (0.8 NA Plan-APO, Zeiss) with an *x–y* and *z* resolution of 0.32 and 1 µm, respectively. For analysis of the spine density and morphology, images were acquired with the Olympus system BX61WI FluoView 1000 (FV1000, Olympus) using a 40× oil immersion objective (1.3 NA U PlanFL N, Olympus) with zoom 4, with a *x–y* resolution of 0.138 µm and sectioned in the *z*-direction spaced 0.3 µm apart.

To acquire the neuronal morphology of GABAergic neurons in primary hippocampal and cortical cultures fluorescent images of parvalbumin-, calbindin- and calretinin-positive neurons were taken using the Axioplan 2 imaging microscope with a 20× objective (0.8 NA Plan-APO, Zeiss) with an *x–y* and *z* resolution of 0.32 and 1 µm, respectively. For the medium spiny neurons of the striatum images of Ctip2-positive neurons in cortico-striatal cultures were taken using the Axioplan 2 imaging microscope with a 20× objective (0.8 NA Plan-APO, Zeiss) with an *x–y* and *z* resolution of 0.32 and 1 µm, respectively. The positivity to CTIP2 was complemented with an observation of the dendritic morphology. CTIP2-positive neurons were selected as medium spiny neurons only when their dendritic length from the soma did not exceed 300 µm, they had a small and round cell body as well as low spine density with thin and long spines to clearly distinguish them from the cortical neurons also present in these cultures. For the morphological analysis of pyramidal cortical and hippocampal neurons images of mCherry-positive neurons clearly showing a bipolar dendritic tree and one long "apical" dendrite were taken using the Axioplan 2 imaging microscope with a 20× objective (0.8 NA Plan-APO, Zeiss) with an *x–y* and *z* resolution of 0.32 and 1 µm, respectively. For the analysis of dendritic spine density, dendritic stretches of mCherry-expressing primary neurons were imaged at the Axioplan 2 imaging microscope using a 63× objective (1.4 N.A., Zeiss) and optical sections were spaced 0.5 µm apart with a *x–y* resolution of 0.1 µm. To examine the BDNF-TrkB signaling pathway, phospho-TrkB immunoreactivity was acquired by confocal sequential scanning with an Olympus system BX61WI FluoView 1000. Images were acquired with a 40× oil immersion objective (1.3 NA U PlanFL N, Olympus), *z*-sectioned 0.5 µm apart with a *x–y* resolution of 0.497 µm. The exposure time was set on the control cells and kept constant.

Morphological analysis

Morphological reconstruction of the neurons was performed using the Neurolucida software (MicroBrightField) and Sholl analysis (Sholl 1953) was applied to quantify the dendritic complexity using Neuroexplorer software

(MicroBrightField). As an index for the total dendritic complexity, the total number of crossings for each cell obtained in the Sholl analysis was used. Density and architecture of dendritic spines were quantified on secondary or tertiary dendrites branches of Dil or mCherry-labeled neurons using the ImageJ software (NIH). The number of dendritic spines was counted using the multipoint tool and the dendritic length were measured by the segmented line tool. Spine density was measured for basal and apical dendrites by determining the number of spines per micrometer of dendritic length. The activation status of the BDNF receptor TrkB was analyzed by measuring the mean fluorescence intensity of the phospho-TrkB signal in neuronal cell bodies (Kellner et al. 2014) using the area selection tool of the ImageJ software (NIH). All treatments were performed in triplicates for each one of at least three independent neuronal preparations. Sample size is currently defined by an a priori power analysis using *G* power with a statistical power $(1-\beta)$ of 0.95. During the analysis the experimentation was blind to the mouse genotype and treatment. Neurons were excluded from the analysis only if they were showing clear signs of degeneration such as fragmented dendrites, retraction bulbs and/or a hairy (growth of numerous short membrane protrusions) soma. The statistical significance was determined by using an unpaired two-tailed Student's *t* test and a one-way ANOVA followed by a post hoc Tukey's multiple comparison test for the analysis of more than two experimental conditions. Kolmogorov–Smirnov test was use to evaluate statistical significance for the cumulative distribution of dendritic spine density. The analysis was performed with Microsoft Excel and GraphPad Prism 5 software. All data shown are represented as mean ± SEM. Asterisks indicate the statistical significance levels as $*p<0.05$; $**p<0.01$; $***p<0.001$.

Results

Previous work using a conditional knock-out mouse essentially lacking BDNF throughout the neurons of the CNS (*cbdnf ko*) revealed a surprising selectivity in the role of BDNF in modulating neuronal architecture within different brain areas (Rauskolb et al. 2010). Indeed, while medium spiny neurons of the striatum strongly depend on BDNF for their development hippocampal pyramidal neurons are not significantly affected by a global BDNF deprivation. The question of whether these observations derive from an area or a cell type-specific activity of BDNF and the molecular mechanisms mediating the differential responsiveness to BDNF of different neuronal populations remained so far elusive.

cbdnf ko GABAergic interneurons show marked alterations in their dendritic architecture

First a possible cell type-specific activity of BDNF in modulating dendritic architecture was addressed by analyzing the morphology of GABAergic interneurons derived from the hippocampus or the cerebral cortex upon BDNF depletion. To this aim hippocampal and cortical primary hippocampal cultures prepared from BDNF floxed mice were transduced or not with lentiviruses to express Cre-recombinase (Ubc GRIG) upon preparation. The dendritic architecture of different GABAergic interneuron types was analyzed at 21DIV in control and BDNF-depleted (BDNFΔ) hippocampal cultures. The different interneuron subtypes were identified by their immunoreactivity to different calcium-binding proteins. These experiments revealed that in comparison to control (grey), parvalbumin-(PV), calbindin-(Calb) and calretinin-positive (Calr) GABAergic interneurons in BDNF-depleted (red) primary hippocampal cultures were markedly smaller (Fig. 1a, d, g). Total dendritic complexity was determined by Sholl analysis and found to be significantly reduced by ~ 50% upon BDNF depletion in all types of GABAergic interneuron analyzed (Fig. 1b, e, h inserts; $p<0.001$; PV: 347.0 ± 36.19 vs. 181.3 ± 7.20, Calb: 214.5 ± 7.52 vs. 99.04 ± 5.14, Calr: 203.5 ± 8.11 vs. 96.18 ± 5.33 intersections). When the number of intersections was plotted against the distance from the cell body, a significant reduction in length and complexity could be observed especially for the distal portion of the dendritic tree of BDNF-depleted GABAergic hippocampal interneurons (Fig. 1b, e, h; PV: $p<0.001$ $F_{1,69}=18.40$; Calb: $p<0.001$ $F_{1,32}=6.428$; Calr: $p<0.001$ $F_{1,30}=11.36$). Moreover, treating BDNF-depleted parvalbumin-positive hippocampal interneurons during the entire culturing time with recombinant BDNF resulted in the complete rescue of their dendritic complexity (orange, Fig. 1b; PV: $p<0.001$ $F_{1,50}=16{,}42$; total complexity 450.8 ± 36.19, $p<0.001$ to control and to cbdnf ko). GABAergic interneurons from cortical primary cultures depleted of BDNF showed also a significant reduction in total dendritic complexity (Fig. 1c, f, i inserts; $p<0.01$ for PV and Calr, $p<0.001$ for Calb; PV: 290.6 ± 24.05 vs. 194.7 ± 17.77, Calb: 178.6 ± 14.34 vs. 98.56 ± 8.31, Calr: 194.0 ± 15.91 vs. 134.3 ± 9.74 intersections). When the number of intersections was plotted against the distance from the cell body, a significant reduction in length and complexity could be observed especially for the distal portion of the dendritic tree of BDNF-depleted parvalbumin- and calretinin-positive interneurons (Fig. 1c, i; PV: $p<0.01$ $F_{1,18}=15.04$; Calr: $p<0.01$ $F_{1,15}=10.51$) and both proximal and distal for calbindin-positive cortical interneurons (Fig. 1f Calb:

$p < 0.001$ $F_{1,14} = 9.148$). Thus, independently of their subtype all interneurons showed a similar reduction in dendritic complexity after depletion of BDNF.

Taken together these observations indicate that the postnatal development of the dendritic architecture of several subtypes of GABAergic interneurons in different brain areas strongly depends on BDNF suggesting a cell type-specific rather than an area-specific activity of BDNF in the postnatal CNS.

Minimal morphological alterations in *cbdnf* ko glutamatergic neurons in hippocampal and cortical primary cultures

Primary hippocampal and cortical cultures were used to gain better mechanistic insights into the role of BDNF/TrkB signaling in controlling neuronal architecture. We started by validating the in vitro system by analyzing the dendritic architecture of excitatory neurons in control and BDNF-depleted primary hippocampal cultures and comparing it to the phenotype previously observed in vivo. To this aim pyramidal neurons in control and BDNF-depleted DIV21 hippocampal cultures were transfected with an expression plasmid for mCherry and their positivity or negativity for the Ubc CRIG virus was confirmed by the presence or absence of eGFP. These experiments revealed no difference in total dendritic complexity (Fig. 2a insert, 242.5 ± 10.32 vs. 239.2 ± 16.32 intersections) as well as in the distribution of complexity relative to the distance from the soma (Fig. 2a, b) between control (grey) and BDNF-depleted (red) cultures (confirming in vivo results from, e.g., Rauskolb et al. 2010). Moreover, while BDNF treatment during the entire culturing time did not affect total dendritic complexity in BDNF-depleted neurons (Fig. 2b′, orange, 239.9 ± 7.44 intersections) it resulted in a significant increase in dendritic complexity (Fig. 2b′, blue, 298.8 ± 14.22 intersections, $p < 0.01$ versus control) when performed in control neurons. We next analyzed dendritic spine density and morphology and could not observe any obvious alteration (Fig. 2c, d, Suppl. Figure 1 and Table 1). Indeed, analyzing the density of dendritic spines in second-order dendritic branches of BDNF-depleted hippocampal pyramidal neurons did not reveal any difference when compared to control conditions (Fig. 2c, c′; 0.91 ± 0.02 vs. 0.91 ± 0.01 spines/µm, Suppl. Figure 1 and Table 1). A 3-week BDNF treatment did not influence spine density in BDNF control and depleted hippocampal neurons (Fig. 2c′; blue, 0.93 ± 0.02 and grey, 0.94 ± 0.01 spines/µm, Suppl. Figure 1A and Table 1). Next dendritic spines were divided into three different subtypes (mushroom, thin or stubby) depending on their length and their head/neck width ratio as previously described (Rauskolb et al. 2010; Zagrebelsky et al. 2010). When the distribution of dendritic spine types was compared, neurons from BDNF-depleted cultures (red) showed a significant reduction in the proportion of mushroom spines (Fig. 2d, $p < 0.001$; 51.3 ± 2.00 vs. 36.67 ± 1.44%) with a correspondingly higher proportion of thin spines (Fig. 2d, $p < 0.001$; 14.88 ± 1.37 vs. 31.16 ± 1.73%). No changes were observed in the proportion of stubby spines (Fig. 2d; 33.99 ± 2.11 vs. 32.82 ± 1.39%). Interestingly, the dendritic spine type distribution observed in neurons from control or BDNF-depleted cultures (orange) treated 3 weeks with BDNF did not show any difference when compared to neurons from control cultures (Fig. 2d, blue, 54.39 ± 2.26, 14.18 ± 0.82 and 31.42 ± 2.20; grey; 53.77 ± 1.25, 16.12 ± 1.14 and 30.10 ± 1.07%). Next the effects of a BDNF depletion were analyzed also for pyramidal neurons in cortical primary cultures (Fig. 2e). As observed for hippocampal pyramidal neurons also for cortical pyramidal neurons both dendritic complexity (Fig. 2f, f′; 214.5 ± 14.53 vs. 199.5 ± 18.35 intersections) as well as dendritic spine density (Fig. 2g, g′; 0.97 ± 0.05 vs. 1.00 ± 0.05 spines/µm, Suppl. Figure 1B and Table 1) in BDNF-depleted cultures (red) did not differ from the one of control cultures (grey). However, the distribution of dendritic spine types of cortical neurons showed an identical shift as in BDNF-depleted hippocampal cultures. Indeed, while significantly less mushroom spines could be observed upon BDNF depletion (Fig. 2h; red; $p < 0.05$; 80.59 ± 5.49 vs. 59.92 ± 4.07%), the proportion of thin spines was significantly increased (Fig. 2h, $p < 0.01$; 20.47 ± 4.57 vs. 30.06 ± 2.94%) compared to control cultures (grey). No alterations could be observed in the proportion of stubby spines (Fig. 2h; 8.92 ± 2.08 vs. 10.00 ± 2.23%). This observation indicates that in both cortical and hippocampal pyramidal neurons in vitro, as already observed in vivo BDNF expression is crucial for the development of the mature spine type distribution but not for dendritic complexity and spine density. Indeed, application of BDNF specifically rescues spine type distribution without affecting the other aspects of dendritic architecture.

In order to assess whether the effect of BDNF depletion observed in vivo on striatal medium spiny neurons could be observed in the in vitro system the dendritic architecture of mCherry-expressing medium spiny neurons, defined by their positivity to Ctip2 was compared in mix cortico-striatal cultures transduced or not with Ubc CRIG. The experiments showed that compared to medium spiny neurons in control cultures (grey), those in BDNF-depleted preparations were markedly smaller (red; Fig. 2i). Indeed, total dendritic complexity determined by Sholl analysis was significantly lower in BDNF-depleted medium spiny neurons (red, MSN) when compared to control ones (Fig. 2k *t*; grey; $p < 0.001$; 147.2 ± 9.43 vs. 78.73 ± 6.12 intersections). Moreover,

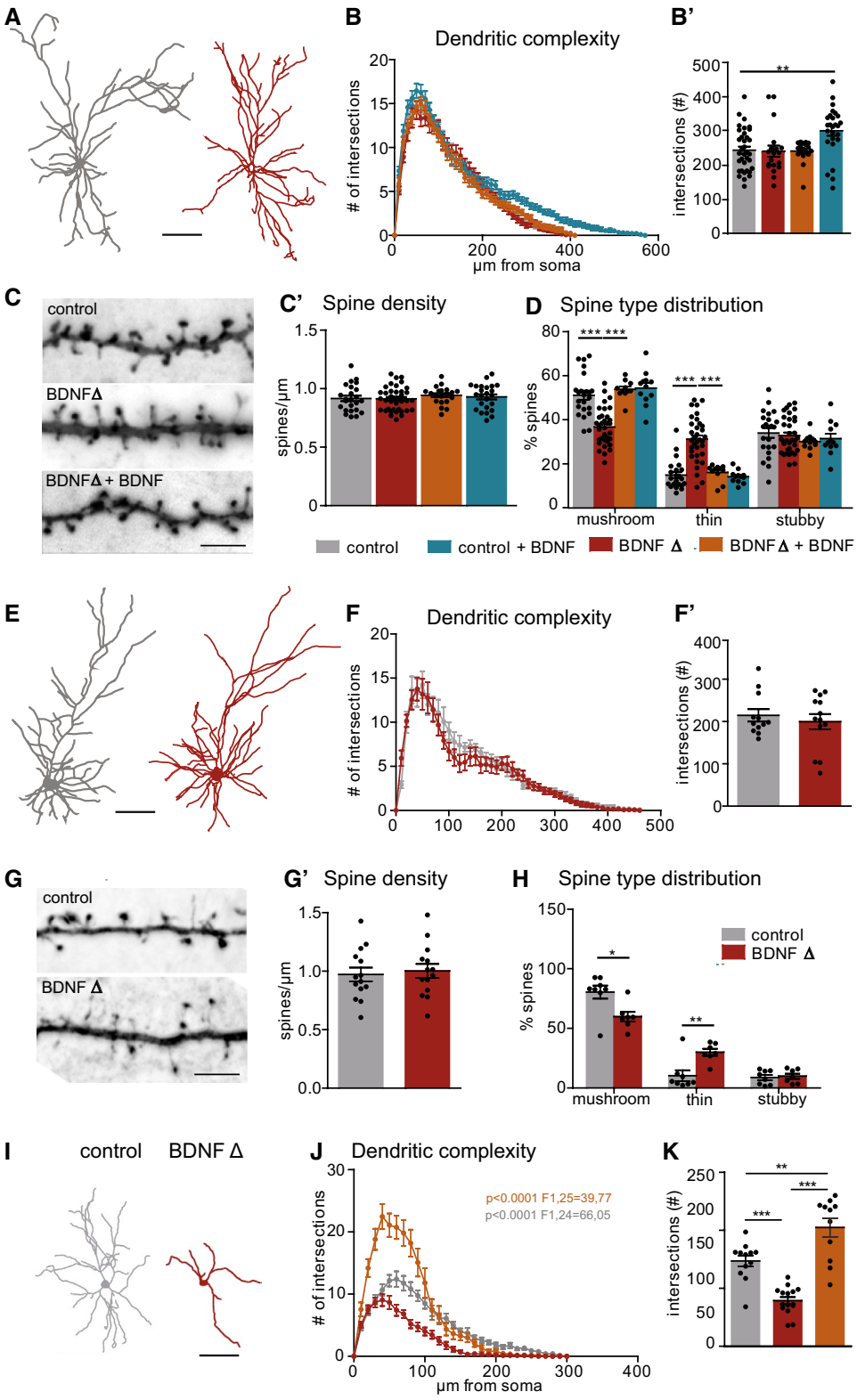

when the number of dendritic intersections was plotted against the distance from the cell body dendritic complexity of MSN was found to be significantly lower in BDNF-depleted cultures (red), especially for the more distal portion when compared to control cultures (Fig. 2j; grey; $p < 0.01$ $F_{1,25} = 6.47$). Treatment with recombinant BDNF of BDNF-depleted MSN (orange) resulted in the complete rescue of the dendritic phenotype with

◂**Fig. 2** Role of BDNF in regulating neuronal architecture and dendritic spine morphology of cultured hippocampal and cortical pyramidal neurons and medium spiny neurons of the striatum. **a** Representative tracing showing the morphology of pyramidal neurons from control (grey) and BDNF-depleted (red BDNFΔ) primary hippocampal cultures. Scale bar 100 µm. **b** Graph showing the Sholl analysis where the number of intersections is plotted against the distance from the cell body and total dendritic complexity (**b′**) of control (grey, $n=35$), BDNF-depleted (red, BDNFΔ, $n=19$), BDNF-depleted neurons treated with BDNF (orange, BDNFΔ + BDNF, $n=18$) as well as control neurons treated with BDNF (blue, control + BDNF, $n=26$) in primary hippocampal pyramidal cultures. **c** Confocal images showing representative stretches of apical dendrites from hippocampal pyramidal primary neurons of all treatments. Scale bar 10 µm. **c′** Graph showing dendritic spine density of control (grey, $n=24$), BDNF-depleted (red, BDNFΔ, $n=39$), BDNF-depleted treated with BDNF (orange, BDNFΔ + BDNF, $n=20$) and control treated with BDNF (blue $n=24$) hippocampal pyramidal primary neurons. **d** Graph showing the distribution of different dendritic spines (mushroom, thin and stubby) in control (grey. $n=23$), BDNF-depleted (red, BDNFΔ, $n=34$), BDNF-depleted neurons treated with BDNF (orange, BDNFΔ + BDNF, $n=11$) and control neurons treated with BDNF (blue, $n=12$) hippocampal cultures. **e** Representative tracing showing the morphology of pyramidal neurons from control (grey) and BDNF-depleted (red BDNFΔ) primary cortical cultures. Scale bar 100 µm. **f** Graph showing the Sholl analysis where the number of intersections is plotted against the distance from the cell body and total dendritic complexity (**f′**) of control (grey, $n=12$) and BDNF-depleted (red, BDNFΔ, $n=13$) cortical pyramidal primary cultures. **g** Confocal images showing representative stretches of apical dendrites from cortical pyramidal primary neurons of all treatments. Scale bar 10 µm. **g′** Graph showing dendritic spine density of control (grey, $n=14$) and BDNF-depleted (red, BDNFΔ, $n=14$) cortical cultures. **h** Graph showing the distribution of different dendritic spines (mushroom, thin and stubby) in control (grey, $n=8$) and BDNF-depleted (red, BDNFΔ, $n=7$) cortical pyramidal primary neurons. **i** Representative tracing showing the morphology of medium spiny neurons from control (grey) and BDNF-depleted (red BDNFΔ) primary cortico-striatal co-cultures. Scale bar 100 µm. **j** Graph showing the Sholl analysis where the number of intersections is plotted against the distance from the cell body and total dendritic complexity (**k**) of control (grey, $n=12$) BDNF-depleted (red, BDNFΔ, $n=15$) and BDNF-depleted medium spiny neurons treated with BDNF (orange, BDNFΔ + BDNF, $n=11$) from cortico-striatal primary cultures. *F* values written in grey refer to the control vs. BDNFΔ comparison, those in orange refer to the BDNFΔ versus BDNFΔ + BDNF comparison. All results are presented as mean ± SEM. And statistical significance is shown as follows: $*p<0.05$; $**p<0.01$, $***p<0.001$

a significantly higher complexity than both control and not-treated BDNF-depleted neurons (Fig. 2j, $p<0.001$ to cbdnf ko and $p<0.001$ to control and Fig. 2k; $p<0.001$ 204.8 ± 16.18 intersections).

Taken together the above observations confirm the cell type-specific effects of BDNF suggested by the in vivo analysis. Indeed, while the mature dendritic architecture of GABAergic neurons in different brain areas strongly depends on BDNF availability, hippocampal glutamatergic neurons only show minor alterations in its absence.

TrkB phosphorylation in glutamatergic versus GABAergic neurons of hippocampal primary cultures

The role of BDNF in positively regulating neuronal morphology has been shown to depend on its ability to activate the TrkB receptor (Alonso et al. 2004). To test whether the differential sensitivity to BDNF shown by excitatory versus inhibitory neurons of the hippocampus and cerebral cortex might be due to differences in TrkB receptor activation, we next compared its phosphorylation levels upon BDNF depletion in the two neuron types. Indeed, measure of phosphorylation of distinct tyrosine residues (phospho-TrkB) has been shown to provide a readout for TrkB activation (Segal et al. 1996). Thus, the intensity of phospho-TrkB immunoreactivity was measured in CamKII- (Fig. 3a) or calbindin-positive (Fig. 3c) neurons and compared between control and BDNF-depleted DIV21 primary hippocampal cultures. Upon quantification of TrkB immunoreactivity no differences could be observed for CamKII-positive neurons in BDNF-depleted (red) versus control hippocampal cultures (Fig. 3b; grey; 100 ± 2.41 vs. 100 ± 6.44%). On the contrary, when compared to control (grey) cultures a significantly lower intensity of TrkB immunoreactivity was measured in calbindin-positive interneurons upon BDNF depletion (Fig. 3d; red; $p<0.001$; 100 ± 2.56 vs. 75.76 ± 2.56%).

The data above indicate that while in GABAergic hippocampal interneurons BDNF depletion results in alteration in their dendritic architecture associated to a reduced TrkB activation, in glutamatergic neurons the lack of morphological changes is combined with the maintenance of TrkB activation at control levels.

Possible role of neurotrophin-4/5 in modulating dendritic architecture of BDNF-depleted excitatory hippocampal neurons

The observations above may suggest that the absence of BDNF is compensated specifically in excitatory hippocampal neurons by the activity of a different ligand able to activate the TrkB receptor. Indeed, neurotrophin-4/5 (NT-4/5) has been shown to bind with high specificity to the TrkB receptor (Ip et al. 1992) and is expressed in the mouse hippocampus (Friedman et al. 1998). Thus, we next tested this hypothesis using the application of TrkB receptor bodies (TrkB-Fc) to scavenge NT-4/5 in BDNF-depleted hippocampal primary cultures. When compared to mCherry-expressing neurons under control conditions depletion of BDNF and NT-4/5 did not influence total dendritic complexity (Fig. 4a insert; 242.5 ± 10.42 vs. 244.1 ± 13.10 intersections) as well as the distribution of dendritic complexity relative to the distance from the cell body determined by the Sholl analysis (Fig. 4a).

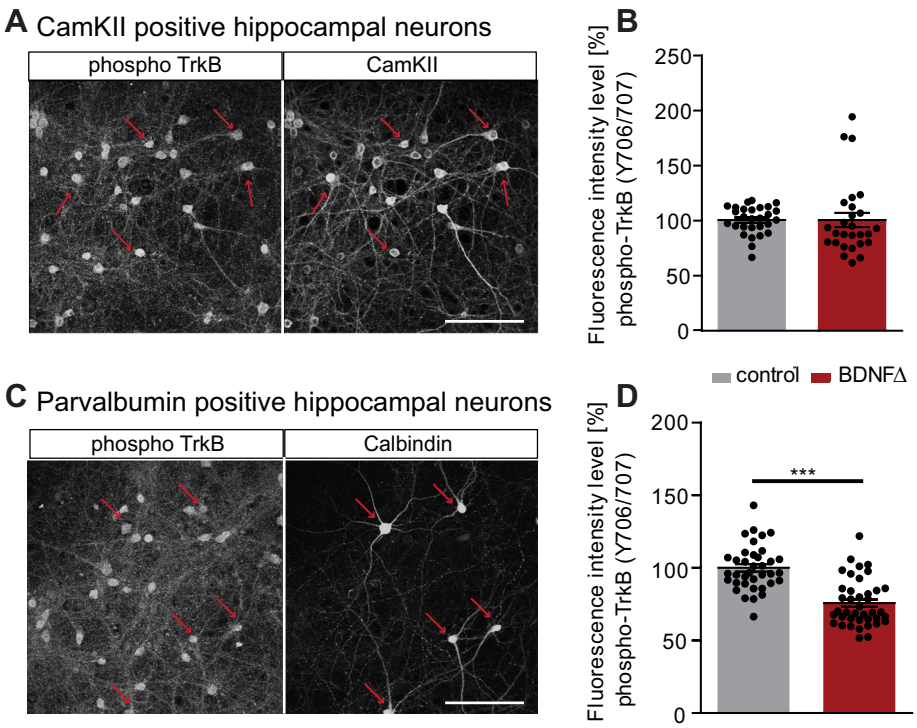

Fig. 3 Quantification of TrkB phosphorylation in excitatory and inhibitory neurons in control and BDNF-depleted hippocampal primary cultures. **a** Confocal images showing immunoreactivity for phospho-TrkB (Y705/Y706; left) and CamKII as a marker for excitatory neurons (right) in primary hippocampal cultures. Scale bar, 100 µm. **b** Quantification of fluorescence intensity for phospho-TrkB in CamKII-positive hippocampal neurons for control (grey, $n=28$) and BDNF depleted (red, BDNFΔ, $n=28$). **c** Confocal images showing immunoreactivity for phospho-TrkB (Y705/Y706; left) and calbindin as a marker for a subtype of inhibitory neurons (right) in primary hippocampal cultures. Scale bar, 100 µm. **d** Quantification of fluorescence intensity for phospho-TrkB in calbindin-positive hippocampal neurons for control (grey, $n=37$) and BDNF depleted (red, BDNFΔ, $n=40$). Data obtained are represented as mean ± SEM and significance is shown as follows: ***$p<0.001$

Similarly, dendritic spine density upon TrkB-Fc treatment in BDNF-depleted cultures was comparable to the one in control, not-depleted hippocampal neurons (Fig. 4b; 0.91 ± 0.02 vs. 0.92 ± 0.02 spines/µm, Suppl. Figure 1C and Table 1). When spine type distribution was analyzed, an equally significant decrease could be observed for mushroom spines both for only BDNF (Fig. 2d) or BDNF and NT-4/5-depleted hippocampal neurons (Fig. 4c, $p<001$; 51.13 ± 1.44 vs. 36.67 ± 1.73 vs. 36.17 ± 1.32%) when compared to the control conditions. In addition, the two treatments resulted in a significant increase in thin (Fig. 4c, $p<0.001$; 14.88 ± 1.37 vs. 31.16 ± 1.73 vs. 32.86 ± 1.16%) and no changes in stubby spines (Fig. 4c; 33.98 ± 2.11 vs. 32.82 ± 1.39 vs. 30.95 ± 1.17%). Next, the levels of TrkB phosphorylation were compared in CamKII-positive neurons between control and BDNF and NT-4/5-depleted hippocampal cultures (Fig. 4d). The quantification of phospho-TrkB immunoreactivity showed no significant differences in the levels of TrkB phosphorylation (Fig. 4e; 100 ± 2.41 vs. 91.41 ± 6.59%) between the two conditions.

Taken together the data so far suggest that the absence of BDNF is compensated specifically in excitatory hippocampal neurons by ligand-independent mechanisms resulting in TrkB phosphorylation.

Role of zinc-dependent TrkB transactivation in modulating dendrite architecture in excitatory hippocampal neurons upon BDNF depletion

The TrkB receptor has been shown to be activated in the absence of BDNF by a variety of stimuli in a process known as transactivation (Jeanneteau and Chao 2006; Puehringer et al. 2013). Previous reports have shown that the divalent cation zinc can transactivate TrkB in cultured cortical neurons and heterologous cells through a BDNF-independent mechanism (Huang et al. 2008). Zinc is expressed at glutamatergic synapses in the hippocampus (Frederickson et al. 2005) and the zinc transporter ZnT-3 has been shown to regulate hippocampal-dependent memory formation (Adlard et al. 2010; Sindreu et al. 2011) suggesting the possibility that a zinc-dependent TrkB transactivation might

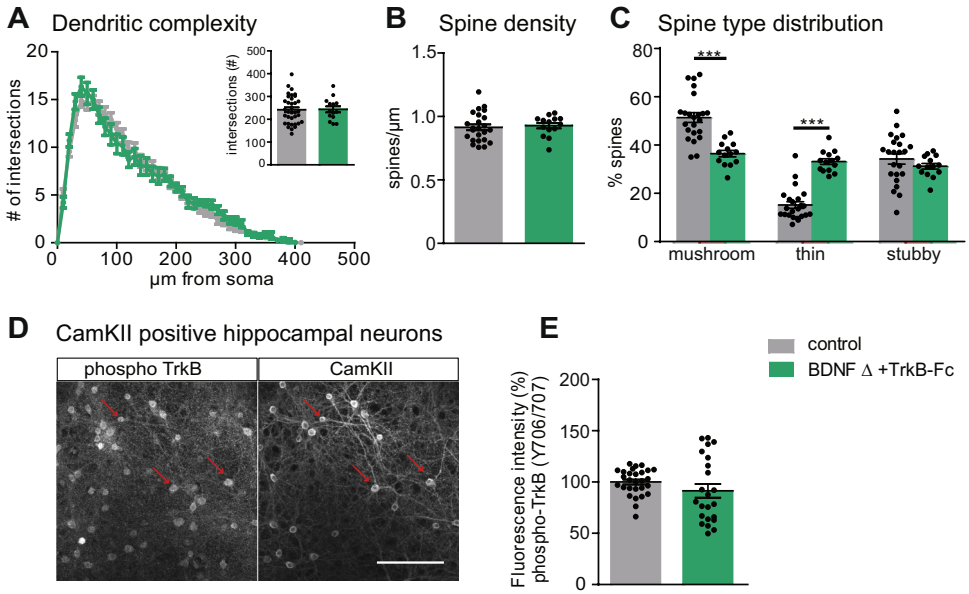

Fig. 4 Role of neurotrophin-4/5 in maintaining neuronal morphology and TrkB receptor phosphorylation in BDNF-depleted primary hippocampal cultures. **a** Graph showing the Sholl analysis where the number of intersections is plotted against the distance from the cell body and total dendritic complexity (insert) of control (grey, $n=35$) and BDNF-depleted neurons treated with TrkB receptor bodies to scavenge NT4/5 (green, BDNFΔ + TrkB-Fc, $n=14$) in hippocampal primary cultures. **b** Graph showing dendritic spine density of control (grey, $n=24$) and BDNF-depleted primary hippocampal cultures treated with TrkB-Fc (green, BDNFΔ + TrkB-Fc, $n=15$). **c** Graph showing the distribution of different dendritic spines (mushroom, thin and stubby) in control (grey, $n=23$) and BDNF-depleted neurons treated with TrkB-Fc (green, BDNFΔ + TrkB-Fc, $n=14$) primary hippocampal cultures. **d** Confocal images showing immunoreactivity for phospho-TrkB (Y705/Y706; left) and CamKII as a marker for excitatory neurons (right) in primary hippocampal cultures. Scale bar, 100 μm. **e** Comparison of fluorescence intensity levels for phospho-TrkB immunoreactivity in control (grey, $n=28$) and BDNF-depleted cultures treated with TrkB-Fc (green, $n=24$). All results are presented as mean ± SEM. Statistical significance is shown as follows: ***$p<0.001$

compensate the BDNF deletion in pyramidal hippocampal neurons. To test this hypothesis the dendritic architecture of mCherry-expressing excitatory neurons was analyzed in control and BDNF-depleted hippocampal cultures treated or not with the zinc chelator Ca EDTA. Upon Ca EDTA treatment both control and BDNF-depleted neurons showed a clear alteration of their dendritic architecture characterized by a very short and simplified dendritic tree (Fig. 5a). Indeed, compared to control neurons both control and BDNF-depleted neurons upon Ca EDTA treatment showed a significantly lower total dendritic complexity (Fig. 5b insert; both $p<0.001$; 242.5 ± 10.42 vs. 149.7 ± 9.06 vs. 106.5 ± 6.29 intersections). Moreover, total dendritic complexity of BDNF-depleted neurons treated with Ca EDTA was significantly lower than the one observed for Ca EDTA-treated WT neurons (Fig. 5b insert; $p<0.01$). Similarly, when dendritic complexity was plotted relative to the distance from the cell body Ca EDTA-treated control and BDNF-depleted pyramidal hippocampal neurons showed a lower complexity throughout the entire dendritic tree (Fig. 5b, $p<0.001$ $F_{2,87}=10.84$). Next, dendritic spine density was analyzed and showed that while Ca EDTA treatment did not influence it in WT neurons, treatment of BDNF-depleted neurons resulted in a significantly reduced dendritic spine density when compared to neurons from control and from Ca EDTA-treated cultures (Fig. 5c; both $p<0.001$; 0.91 ± 0.02 vs. 0.93 ± 0.02 vs. 0.77 ± 0.02 spine/μm, Suppl. Figure 1D and Table 1). The analysis of the distribution of dendritic spine types revealed that when compared to control conditions (Fig. 5d; grey; mushroom 51.13 ± 2, thin 14.88 ± 2.37%) the treatment with Ca EDTA of control neurons (Fig. 5d; blue; mushroom 47.22 ± 0.84, thin 17.93 ± 1.15%) did not influence it. In contrast, application of Ca EDTA to BDNF-depleted hippocampal primary cultures (green) resulted in a significant decrease in the proportion of mushroom spines (Fig. 5d, $p<0.001$; 34.38 ± 1.5%) and a significant increase in thin spines in hippocampal neurons (Fig. 5d, $p<0.001$; Fig. 5d; 32.68 ± 1.54%). These changes were indistinguishable from those observed in pyramidal neurons from not-treated BDNF-depleted hippocampal cultures (Fig. 5d; red; mushroom 36.67 ± 1.44, thin 31.16 ± 1.73). No differences could be observed for the proportion of stubby spines under all conditions (Fig. 5d; 33.98 ± 2.11 vs. 32.84 34.84 ± 1.09 1.39 vs. 34.84 ± 1.09 vs. 32.92 ± 0.82%). In an additional set of experiments Ca EDTA was applied to BDNF-depleted primary hippocampal neurons with or without $ZnCl_2$.

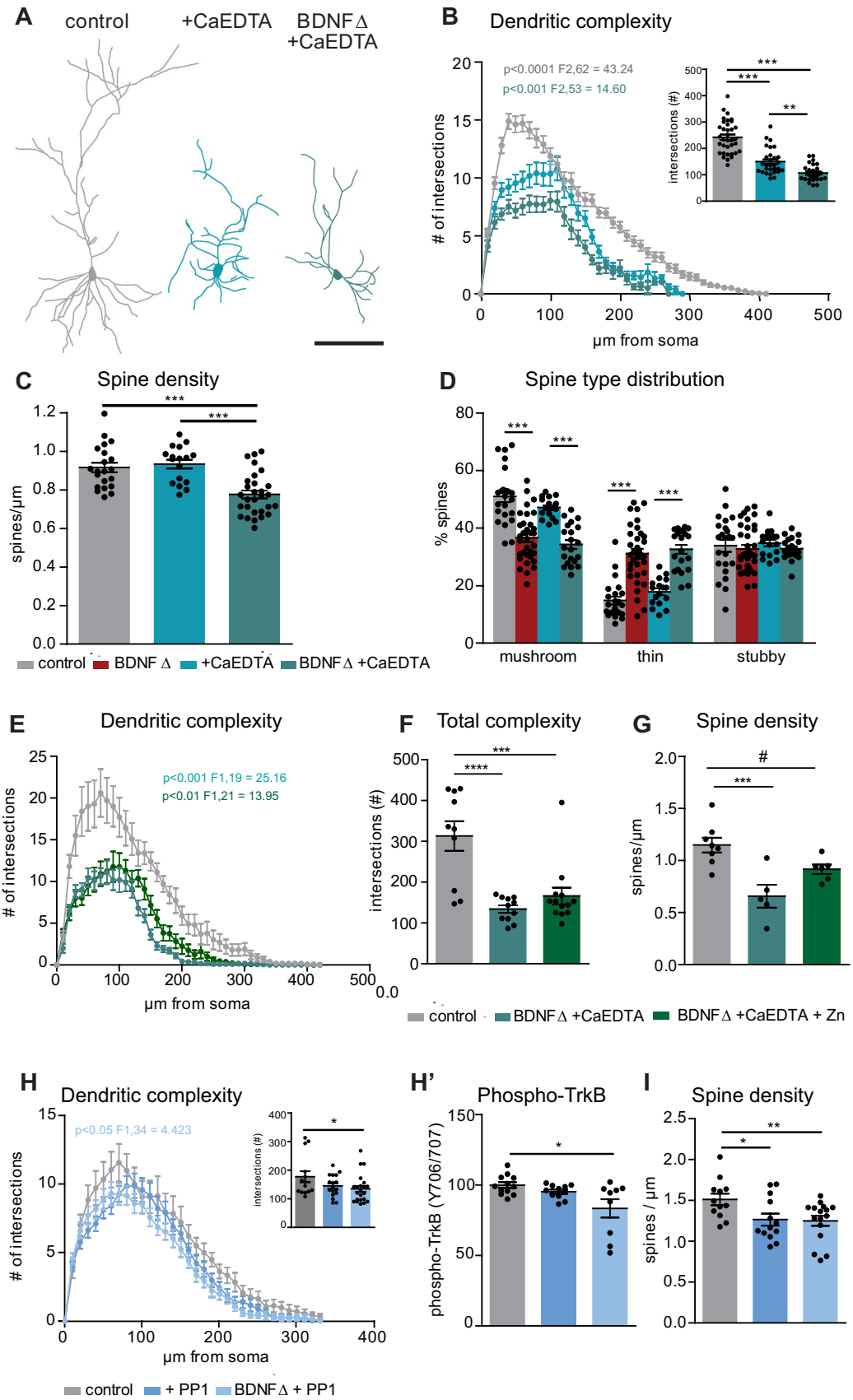
A
control
+CaEDTA
BDNFΔ +CaEDTA
B
Dendritic complexity
p<0.0001 F2,62 = 43.24
p<0.001 F2,53 = 14.60
# of intersections
μm from soma
intersections (#)
C
Spine density
spines/μm
control
BDNF Δ
+CaEDTA
BDNFΔ +CaEDTA
D
Spine type distribution
% spines
mushroom
thin
stubby
E
Dendritic complexity
p<0.001 F1,19 = 25.16
p<0.01 F1,21 = 13.95
# of intersections
μm from soma
F
Total complexity
intersections (#)
G
Spine density
spines/μm
control
BDNFΔ +CaEDTA
BDNFΔ +CaEDTA + Zn
H
Dendritic complexity
p<0.05 F1,34 = 4.423
# of intersections
μm from soma
intersections (#)
control
+ PP1
BDNFΔ + PP1
H'
Phospho-TrkB
phospho-TrkB (Y706/707)
I
Spine density
spines / μm

◂**Fig. 5** Role of ligand-independent TrkB transactivation in regulating dendritic morphology and spine density of primary hippocampal excitatory neurons. **a** Representative tracings comparing the morphology of control (left), Ca EDTA-treated (middle) and BDNF-depleted hippocampal neurons treated with Ca EDTA (right). Scale bar, 100 µm. **b** Graph showing the Sholl analysis where the number of intersections is plotted against the distance from the cell body and total dendritic complexity (insert) of control (grey, $n=29$), Ca EDTA-treated control (blue, +Ca EDTA, $n=29$) and BDNF-depleted neurons treated with Ca EDTA (green, BDNFΔ + Ca EDTA, $n=26$) in hippocampal primary cultures. F values written in grey refer to the control versus + Ca EDTA comparison, those in blue refer to the + Ca EDTA versus BDNFΔ + Ca EDTA comparison. **c** Graph showing dendritic spine density of control (grey, $n=21$), control (blue, + Ca EDTA, $n=17$) and BDNF-depleted (green, BDNFΔ + Ca EDTA, $n=26$) hippocampal primary neurons treated with Ca EDTA. **d** Graph showing the distribution of different dendritic spines (mushroom, thin and stubby) in control (grey, $n=23$), BDNF-depleted (red, BDNFΔ, $n=34$), control (blue, + Ca EDTA, $n=17$) and BDNF-depleted (green, BDNFΔ + Ca EDTA, $n=21$) primary hippocampal neurons treated with Ca EDTA. **e** Graph showing the Sholl analysis where the number of intersections is plotted against the distance from the cell body and total dendritic complexity (**f**) of control (grey, $n=10$), BDNF-depleted primary hippocampal neurons treated with Ca EDTA (green, BDNFΔ + Ca EDTA, $n=11$) or with Ca EDTA and $ZnCl_2$ (dark blue, BDNFΔ + CaEDTA + Zn, $n=13$). F values written in grey refer to the control versus + Ca EDTA comparison, those in green refer to the + Ca EDTA versus BDNFΔ + Ca EDTA and Zn comparison. **g** Graph showing dendritic spine density of control (grey, $n=21$), BDNF-depleted neurons treated Ca EDTA (green, BDNFΔ + Ca EDTA, $n=19$) or with Ca EDTA and $ZnCl_2$ (dark blue, BDNFΔ + CaEDTA + Zn, $n=21$) in primary hippocampal cultures. **h** Graph showing the Sholl analysis where the number of intersections is plotted against the distance from the cell body and total dendritic complexity (insert) of control (grey, $n=14$), control treated with the SFK inhibitor PP1 (dark blue, + PP1, $n=17$) and BDNF-depleted neurons treated with PP1 (light blue, BDNFΔ + PP1, $n=22$) in hippocampal primary cultures. F values written in light blue refer to the control BDNFΔ + PP1 comparison. **h′** Quantification of TrkB phosphorylation level in control hippocampal neurons non-treated (grey, $n=12$) and treated (dark blue, $n=14$) with the SFK inhibitor PP1 as well as BDNF-depleted neurons treated with SFK inhibitor (light blue, $n=9$). **i** Graph showing dendritic spine density of control (grey, $n=12$), control neurons treated with SFK inhibitor PP1 (dark blue, + PP1, $n=11$) and BDNF-depleted neurons treated with PP1 (light blue, BDNFΔ + PP1, $n=13$) primary hippocampal cultures. All results are presented as mean ± SEM, statistical significance is shown as follows $*p<0.05$; $**p<0.01$, $***p<0.001$

While the treatment did not significantly rescue dendritic complexity (Fig. 5e; dark blue BDNFΔ + Ca EDTA + Zn) resulting in a significantly lower complexity distribution (Fig. 5e, $p<0.001$, $F_{1,19}=17.47$ for ctrl vs. Ca EDTA and $F_{1,21}=20.82$ for ctrl vs. Ca EDTA + Zn) and total complexity (Fig. 5f; ctrl 313.0 ± 36.18, Ca EDTA 134.0 ± 9.02 and Ca EDTA + Zn 166.0 ± 20.57 intersections) than controls, it partially rescued dendritic spine density (Fig. 5g; ctrl 1.49 ± 0.07 vs. BDNFΔ 0.65 ± 0.11; $p<0{,}001$ and BDNFΔ + Zn 0.91 ± 0.04, Suppl. Figure 1E and Table 1). Finally, in a set of BDNF-depleted hippocampal cultures the zinc transporter ZnT-3 (Schen et al. 2007) was downregulated via shRNA expression starting at DIV 7. ZnT-3 is known to be localized at glutamatergic synapses (Wenzel et al. 1997) and its deletion prevents zinc uptake at synaptic vesicles (Cole et al. 1999). Indeed, the targeted deletion of ZnT-3 results in reduced zinc levels in fibers normally containing zinc (Cole et al. 1999; Linkous et al. 2008). While the Sholl analysis confirmed the absence of a dendritic phenotype in BDNF-depleted (red) mCherry-expressing hippocampal pyramidal neurons when compared to the control (grey), downregulation of ZnT-3 in BDNF-depleted hippocampal neurons resulted in a significantly reduced dendritic complexity throughout the entire dendritic tree (Fig. 6a, blue). Indeed, while total dendritic complexity was not different between control (Fig. 6b, grey, 337.1 ± 27.61) and BDNF-depleted (Fig. 6b, red, 281.2 ± 35.49) pyramidal hippocampal neurons, it was significantly lower in BDNF-depleted neurons upon ZnT-3 downregulation (Fig. 6b, blue 80.33 ± 22.05, $p<0.0001$ vs. control and $p<0.001$ vs. BDNFΔ). Next, dendritic spine density was analyzed and showed that while BDNF-depleted neurons (Fig. 6c red, Suppl. Figure 1G and Table 1) did not show a significantly reduced dendritic spine density when compared to neurons from control (Fig. 6c, grey, Suppl. Figure 1G and Table 1), upon ZnT-3 downregulation in BDNF-depleted neurons spine density was significantly reduced (Fig. 6c; blue, both $p<0.05$; 1.24 ± 0.09 vs. 1.20 ± 0.16 vs. 0.57 ± 0.06 spine/µm, Suppl. Figure 1G and Table 1).

Our results so far indicate that while in hippocampal pyramidal neurons distribution of dendritic spine types depends purely on BDNF availability, zinc might indeed be involved in rescuing the dendritic architecture and dendritic spine density in BDNF-depleted cultures. Src family kinases (SFK) have been shown to be required for zinc-induced phosphorylation of Tyr-706 residue of TrkB (Huang et al. 2008; Huang and McNamara 2010). Thus, we next tested whether inhibition of Src kinases via the application of the SFK inhibitor PP1 influences dendritic complexity and spine density in pyramidal hippocampal neurons. When compared to a treatment with the inactive analog PP3 (grey) inhibition of SFK resulted in a reduced dendritic complexity both in control and BDNF-depleted neurons (Fig. 5h). However, this became significant only for PP1-treated BDNF-depleted neurons (Fig. 5h, $p<0.05$; 177.3 ± 19.28 vs. 145.2 ± 11.92 vs. 134.7 ± 10.56 intersections). Interestingly, while TrkB phosphorylation was only slightly reduced in PP1-treated control neurons (Fig. 5h′; blue; 95.35 ± 1.47%), it was significantly lower in PP1-treated BDNF-depleted neurons (Fig. 5h′; $p<0.05$; light blue; 83.43 ± 6.53%) when compared to the control conditions (Fig. 5h′; grey; 100 ± 2.02%). The analysis of dendritic spine density revealed a significant decrease both in control (Fig. 5i; blue; $p<0.05$; 1.26 ± 0.07 spines/µm, Suppl. Figure 1F and Table 1) and BDNF-depleted (Fig. 5i; light blue; $p<0.01$; 1.24 ± 0.06 spines/µm, Suppl. Figure 1F and Table 1) hippocampal pyramidal

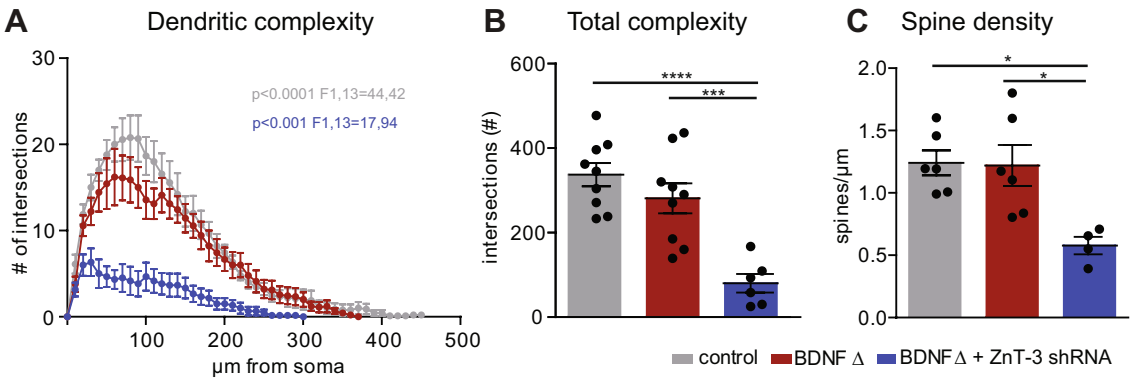

Fig. 6 Role of the zinc transporter ZnT-3 in modulating neuronal architecture and dendritic spine density for pyramidal hippocampal neurons in vitro. **a** Graph showing the Sholl analysis where the number of intersections is plotted against the distance from the cell body and total dendritic complexity (**b**) of control (grey, $n=9$), BDNF-depleted (red, BDNFΔ, $n=9$) and BDNF-depleted neurons transfected with shRNAs for ZnT-3 (blue, BDNFΔ + shRNA ZnT-3, $n=6$) in hippocampal primary cultures. **c** Graph showing dendritic spine density of control (grey, $n=6$), BDNF-depleted (red, BDNFΔ, $n=6$) and BDNF-depleted neurons transfected with shRNAs for ZnT-3 (blue, BDNFΔ + shRNA Znt-3, $n=4$) hippocampal primary neurons treated with Ca EDTA. All results are presented as mean ± SEM, statistical significance is shown as follows $*p<0.05$; $**p<0.01$, $***p<0.001$

neurons treated with PP1 compared to controls (Fig. 5i; grey; 1.51 ± 0.07 spines/μm, Suppl. Figure 1F and Table 1).

Taken together these data suggest that zinc-mediated TrkB transactivation might indeed, at least partially contribute to maintain dendritic spine density in BDNF-depleted pyramidal neurons.

Morphological analysis of cortical pyramidal neurons and granule neurons of the dentate gyrus in *cbdnf ko* mice

In view of the mild alterations observed for hippocampal pyramidal neurons both in vivo in the *cbdnf* ko mice and in vitro in BDNF-depleted primary cultures, we set out to explore if pyramidal neurons are in general only mildly affected if BDNF is missing. Very early on after the discovery of BDNF, it was shown, that in the ferret developing cortex, the application of BDNF does increase dendritic complexity reviewed in (McAllister et al. 1999). However, an effect of a gain-of-function approach could not be observed in hippocampal primary cultures (Kellner et al. 2014). In addition, preparation techniques (Danzer et al. 2004) and culture conditions (Chapleau et al. 2008) have been shown to influence the level of expression as well as the cellular response to BDNF, possibly confounding the analysis of the role of endogenous BDNF under culture conditions. We therefore analyzed the morphology of single pyramidal neurons from the cortical Layer II/III and Layer V of *cbdnf ko* mice. Pyramidal neurons were labeled with Dil in 8-week-old WT and *cbdnf ko* mice, virtually lacking BDNF throughout the CNS (Rauskolb et al. 2010). When qualitatively compared with WT neurons no obvious alterations in the gross dendritic architecture could be observed for both Layer II/III (Fig. 7a) and Layer V pyramidal neurons (Fig. 7d). This qualitative impression was confirmed comparing total dendritic complexity analyzed by Sholl analysis. Due to their different connectivity the apical and basal dendrites were analyzed separately. Mutant Layer II/III pyramidal neurons showed only a slightly, but not significant reduction in total complexity for the apical dendrite (Fig. 7b insert; 106.38 ± 7.57 vs. 83.66 ± 21.4 intersections) and no difference for the basal dendrite when compared to WT neurons (Fig. 7c insert; 114.07 ± 8.95 vs. 108.12 ± 11.21 intersections). Similarly, no significant differences in total dendritic complexity could be observed both for the apical and basal dendrites of Layer V mutant and WT pyramidal neurons (Fig. 7e, f; apical 109.5 ± 9.24 vs. 109.7 ± 11.34; basal 98.27 ± 11.38 vs. 100.11 ± 12.01 intersections). A more detailed Sholl analysis performed by plotting the number of dendritic intersections against the distance from the cells body showed only a mild reduction in the most distal portion of the apical dendrite of Layer II/III mutant neurons (Fig. 7b) when compared to WT Layer II/III neurons. No other differences in dendritic complexity could be observed between WT and *cbdnf ko* cortical neurons (Fig. 7c, e, f). Analysis of dendritic spine density showed no differences between WT and *cbdnf ko*-derived pyramidal neurons both for cortical Layer II/III (Fig. 7g; 1.15 ± 0.07 vs. 1.16 ± 0.06 spines/μm, Suppl. Figure 2A and Table 1) and Layer V (Fig. 7h; 1.12 ± 0.10 vs. 1.21 ± 0.08 spines/μm, Suppl. Figure 2B and Table 1). However, when the distribution of dendritic spine types was analyzed a significant decrease in mushroom spines (Fig. 7i, $p<0.05$; 48.53 ± 2.95 vs. 38.42 ± 2.58%) associated to a significant increase in thin spines (Fig. 7i, $p<0.01$; 25.99 ± 1.56 vs.

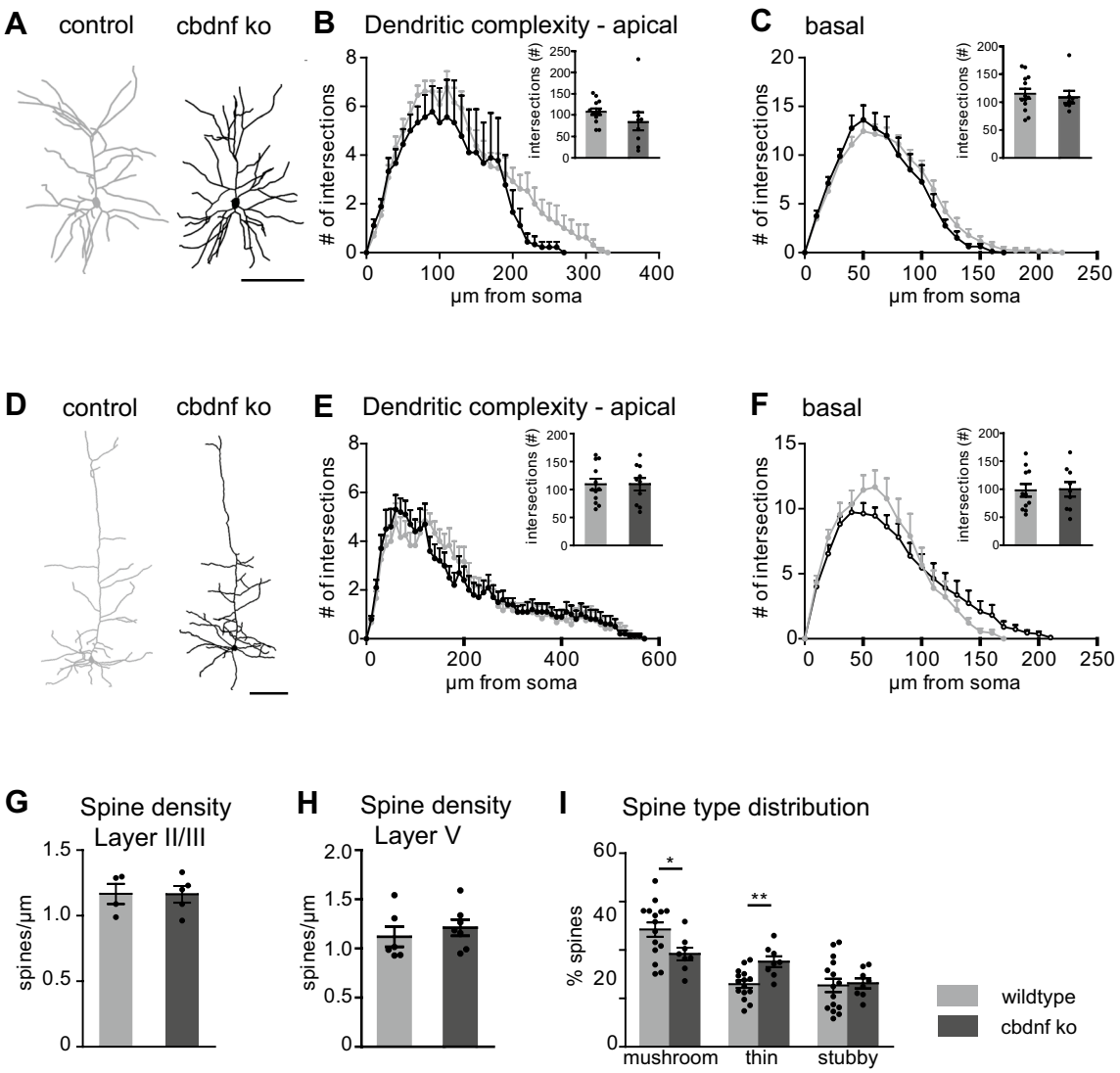

Fig. 7 Analysis of neuronal architecture and dendritic spine density for pyramidal neurons from Layer II/III and Layer V of the somatosensory cortex of wild type and c*bdnf* knock-out mice. Representative tracings showing the morphology of Dil-labeled cortical Layer II/III (**a**) and Layer V (**d**) pyramidal neurons from wild type (light grey) and c*bdnf* ko mice (dark grey). Scale bar, 100 µm. **b, c** Graphs showing Sholl analysis where the intersections are plotted against the distance from the soma and as total dendritic complexity (inserts) of both apical and basal dendrites from wild type (light grey, $n=13$ apical and $n=13$ apical) and c*bdnf* ko (dark grey, $n=9$ basal and $n=8$ basal) pyramidal cortical neurons in Layer II/IIII. **e, f** Graphs showing Sholl analysis where the intersections are plotted against the distance from the soma and as total dendritic complexity (inserts) of both apical and basal dendrites from wild type (light grey, $n=12$ apical and $n=10$ apical) and c*bdnf* ko (dark grey, $n=11$ basal and $n=9$ basal) pyramidal cortical neurons in Layer V. **g** Graphs showing dendritic spine density of wild type (light grey, $n=4$) and c*bdnf* ko mice (dark grey, $n=5$) for neurons in Layer II/III and **h** Layer V ($n=6$ control and $n=7$ cbdnf ko). **f, i** Graph showing the distribution of different spine types for cortical Layer II/III and V of wild type (light grey, $n=15$) and c*bdnf* ko mice (dark grey, $n=8$). All data obtained are presented as mean ± SEM, statistical significance is shown as follows: $*p<0.05$; $**p<0.01$

35.26 ± 2.25%) could be observed in mutant vs. WT cortical pyramidal neurons (Fig. 7i). This result very much resembles the data we obtained from hippocampal pyramidal neurons in vivo (Rauskolb et al. 2010) and from our in vitro results (Fig. 2). These results indicate that BDNF deprivation in vivo fails to cause major alterations in the dendritic architecture of pyramidal cortical neurons.

Taken together our results so far strongly suggest that in vitro as well as in vivo excitatory and inhibitory neurons from different brain regions show different levels of sensitivity to BDNF depletion indicating a cell type-specific role of BDNF during postnatal development. To confirm this hypothesis, we next analyzed the dendritic architecture of another type of excitatory neurons from the hippocampus,

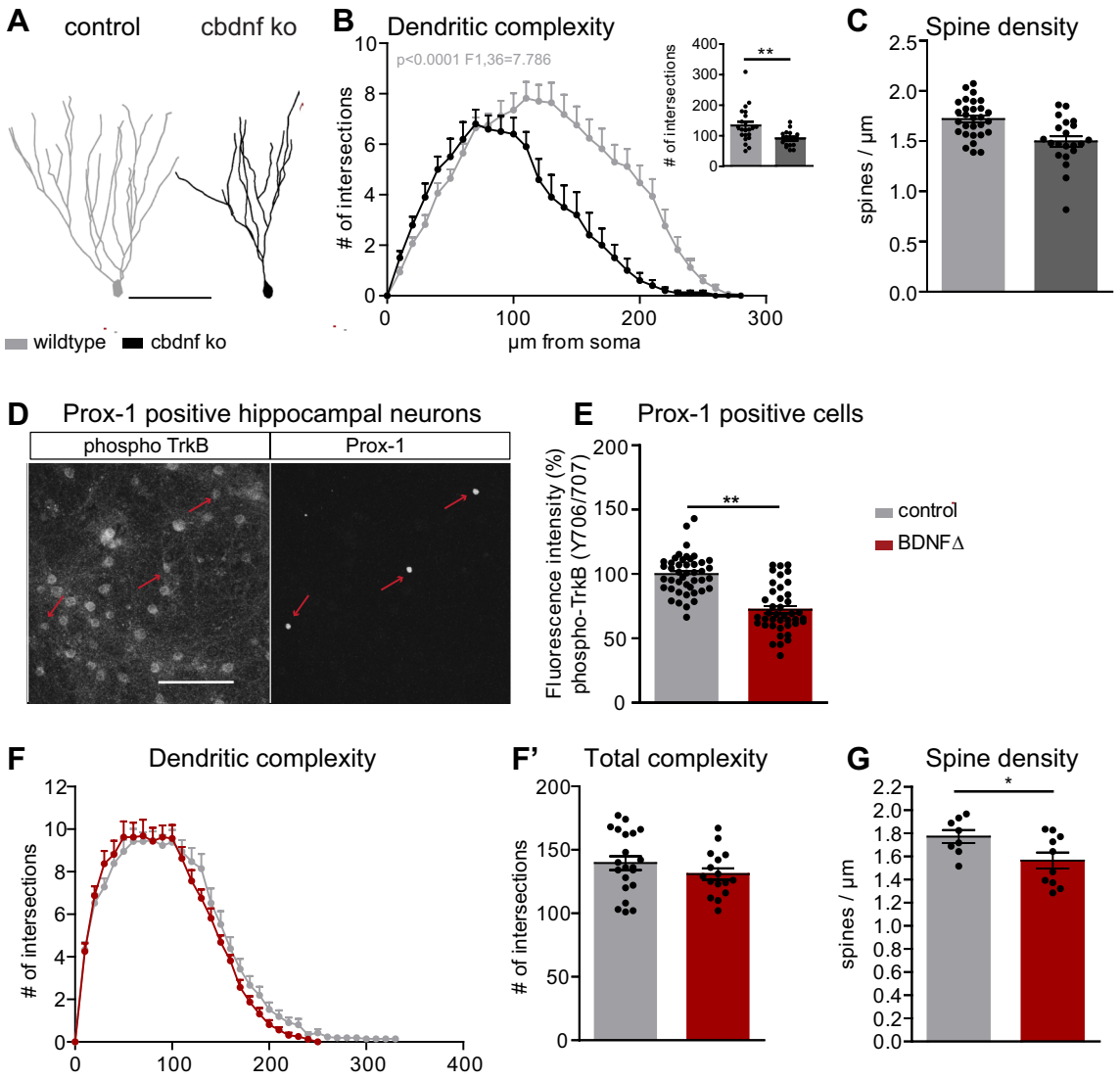

Fig. 8 Neuronal morphology of dentate gyrus granule cells from wild type and *cbdnf* knock-out mice and quantification of TrkB phosphorylation in Prox-1-positive primary hippocampal neurons. **a** Representative tracings showing the morphology of dentate gyrus granule cells in wild type (grey) and *cbdnf* ko mice (black). Scale bar, 100 µm. **b** Graphs showing Sholl analysis where the intersections are plotted against the distance from the soma and as total dendritic complexity (inserts) of Dil-labeled wild type (light grey, $n=22$) and *cbdnf* ko (dark grey $n=16$) granule cells of the hippocampus. **c** Graphs showing dendritic spine density of Dil-labeled wild type (light grey, $n=8$) and *cbdnf* ko (dark grey, $n=10$) granule cells of the dentate gyrus. **d** Confocal images showing immunoreactivity for phospho-TrkB (Y705/Y706; left) and Prox-1 as a marker for granule cells (right) in primary hippocampal cultures. Scale bar, 100 µm. **e** Quantification of TrkB phosphorylation level in control (grey, $n=44$) and BDNF-depleted (red BDNFΔ, $n=41$) Prox-1-positive hippocampal neurons. **f** Graphs showing Sholl analysis where the intersections are plotted against the distance from the soma and as total dendritic complexity (**g**) of mCherry-expressing control (grey, $n=21$) and BDNF-depleted (red, BDNFΔ, $n=16$) Prox1-positive granule cells of the hippocampus. **h** Graphs showing dendritic spine density of mCherry-transfected wild type (grey, $n=8$) and BDNF-depleted (red, BDNFΔ, $n=10$) Prox1-positive granule cells of the dentate gyrus. All results are presented as mean ± SEM, statistical significance is shown as follows*$p<0.05$; **$p<0.01$, ***$p<0.001$

namely granule cells of the dentate gyrus in WT and *cbdnf ko* mice. At a qualitative analysis Dil-labeled mutant granule cells seemed to have a shorter and less complex dendritic tree that WT neurons (Fig. 8a). Indeed, when total dendritic complexity was analyzed it surprisingly resulted to be significantly lower in mutant granule cells than in WT neurons (Fig. 8b insert; $p<0.01$; 133.5 ± 12.22 vs. 90.38 ± 6.7 intersections). Similarly, when the number of intersections was plotted against the distance from the cell body, *cbdnf ko* granule cells showed a significantly lower dendritic complexity, especially in the distal two-thirds of the dendritic tree (Fig. 8b, $p<0.001$ $F_{1,36}=21.90$). Moreover, dendritic spine density was significantly lower in *cbdnf ko* derived than in WT granule cells (Fig. 8c, $p<0.01$;

1.72 ± 0.03 vs. 1.44 ± 0.05 spines/µm, Suppl. Figure 2C and Table 1). Interestingly, TrkB phosphorylation analyzed in granule cells identified by their positivity to Prox-1 was significantly lower in BDNF depleted ($p < 0.01$) than in control primary hippocampal cultures (Fig. 8e; 100 ± 3.18 vs. 80.29 ± 5.11%). Moreover, dendritic architecture and spine density were analyzed in Prox1-positive mCherry-expressing neurons in hippocampal cultures. While dendritic complexity (Fig. 8f, f′, grey control 142.1 ± 8.64, red BDNFΔ 140.7 ± 5.57), did not show any significant alteration, dendritic spine density was significantly lower in BDNF-depleted cells vs. control (Fig. 8g, grey control 1.71 ± 0.05 and red BDNFΔ 1.56 ± 0.06; $p < 0.05$, Suppl. Fig. sD and Table 1).

These results clearly indicate that in contrast to other hippocampal and cortical glutamatergic neurons granule cells of the dentate gyrus depend on BDNF for the postnatal development of their dendritic architecture.

Discussion

Our results give strong evidence for a cell type-specific TrkB signaling in modulating neuronal architecture. Indeed, while BDNF deprivation both in vivo and in vitro fails to cause major alterations in the dendritic architecture of pyramidal hippocampal and cortical neurons, it significantly affects both granule cells of the dentate gyrus as well as cortical and hippocampal inhibitory interneurons, as well as inhibitory neurons in the striatum. The results strongly suggest that in vitro as well as in vivo excitatory pyramidal neurons, granule cells from the DG and inhibitory interneurons from the cortex and hippocampus show different levels of sensitivity to BDNF. Moreover, our results suggest that zinc-dependent, ligand-independent transactivation of TrkB receptors might explain the cell-specific BDNF sensitivity and could possibly compensate the lack of BDNF-mediated signaling specifically in pyramidal cortical and hippocampal neurons.

BDNF modulates neuronal architecture in a cell type-specific manner

Global deprivation of BDNF throughout the entire CNS results in specific reduction in the volume of specific areas of the brain, i.e., the striatum and not in others, i.e., hippocampus and cortex (Rauskolb et al. 2010). The reduction in volume of the striatum in the absence of BDNF is due to a highly significant reduction of the total length and volume of dendrites as well as in dendritic spine density for medium spiny neurons (MSN, Rauskolb et al. 2010), comprising about 90% of the neurons in the striatum. On the other hand, pyramidal neurons of the CA1 area of the hippocampus did not show major alterations in their architecture (Rauskolb et al. 2010). Moreover, BDNF markedly promotes the growth of cultured striatal neurons and of their dendrites, but not of those of hippocampal neurons (Rauskolb et al. 2010), suggesting that the differential responsiveness to BDNF is part of a neuron-intrinsic program but leaving open the question of whether BDNF modulates neuronal architecture in a region- or cell type-specific manner. The results of the current study indicate that in vivo, BDNF specifically regulates the architecture of several subtypes (parvalbumin-, calbindin- and calretinin-positive) of GABAergic neurons of the cortex, hippocampus and striatum, but does not play a major role in this context for pyramidal, glutamatergic neurons within the same regions. These results are in line with previous evidence obtained in vitro indicating that BDNF promotes the phenotype differentiation of GABAergic neurons in hippocampus and striatum (Mizuno et al. 1994; Marty et al. 1996; Ivkovic and Ehrlich 1999; Yamada et al. 2002), facilitates dendritic development of hippocampal GABAergic neurons in culture (Bartrup et al. 1997; Vicario-Abejon et al. 1998; Kohara et al. 2003, 2007; Turrigiano 2007; Hong et al. 2008), increases the density of inhibitory synapses (Marty et al. 2000) or the size of inhibitory terminals (Bolton et al. 2000) of hippocampal neurons. Due to the lack of BDNF synthesis in GABAergic interneurons, it can be concluded that in this context it acts in a paracrine manner. On the other hand, while several in vitro studies also suggested a role for exogenous BDNF in modulating dendritic architecture of pyramidal neurons of the cortex and hippocampus (McAllister et al. 1995, 1996, 1997; Horch et al. 1999; Tyler and Pozzo-Miller 2001, 2003; Ji et al. 2005, 2010; Kellner et al. 2014), we could not reproduce these observations in vivo. However, we did observe a surprising significant reduction in dendritic complexity and dendritic spine density for the granule cells of the dentate gyrus. While this result is in agreement with previous observations showing a role of BDNF in regulating dendritic complexity in the dentate gyrus (Tolwani et al. 2002; Gao et al. 2009; Wang et al. 2015), it does not support our hypothesis of a specific activity of BDNF on inhibitory but not excitatory neurons. On the other hand, several reports indicate that BDNF regulates dendritic development and synaptic formation of postnatal-born dentate gyrus granule neurons (Gao et al. 2009; Waterhouse et al. 2012; Wang et al. 2015) leaving open the possibility that the phenotype observed in the dentate gyrus of c*bdnf* ko mice derives from an activity of BDNF in modulating adult neurogenesis.

TrkB receptor activation

Extensive in vitro and in vivo evidence indicates that BDNF influences neuronal architecture via the activation of the TrkB receptor both in glutamatergic (Horch et al. 1999;

Yacoubian and Lo 2000; Tyler and Pozzo-Miller 2001, 2003; Ji et al. 2005, 2010; Chakravarthy et al. 2006; Kellner et al. 2014) and GABAergic neurons (Mizuno et al. 1994; Widmer and Hefti 1994; Marty et al. 1996; Rutherford et al. 1997; Vicario-Abejon et al. 1998; Seil and Drake-Baumann 2000; Yamada et al. 2002). Activation of TrkB depends upon its dimerization and the consequent phosphorylation of tyrosine residues within its intracellular domain (McAllister et al. 1999; Huang and Reichardt 2001; Minichiello 2009). Thus, measuring phosphorylation of distinct tyrosine residues provides a way to measure TrkB activation (Segal et al. 1996). We observe that while TrkB phosphorylation is significantly reduced within the cell body of BDNF-depleted GABAergic hippocampal neurons as well as in granule cells of the hippocampus, it is not altered within pyramidal neurons both in the hippocampus and in the cortex. Thus, it can be concluded that a BDNF-dependent TrkB activation is required to control dendritic architecture of GABAergic cortical and hippocampal neurons and granule cells of the dentate gyrus. On the other hand, the lack of a reduction in TrkB phosphorylation associated with the limited dendritic phenotype of BDNF-depleted pyramidal neurons indicates the existence of a BDNF-independent activation of TrkB able to compensate for the lack of BDNF and maintain dendritic complexity and spine density specifically for pyramidal neurons in the absence of BDNF both in vitro and in vivo. Moreover, scavenging of both BDNF and NT-4/5, the second ligand for TrkB, did not result in reduced TrkB phosphorylation or dendritic complexity suggesting a neurotrophin-independent mechanism. Indeed, this is in line with previous reports showing TrkB receptor activation in the mossy fiber pathway during epileptogenesis in the absence of BDNF or both NT-4/5 and BDNF (He et al. 2004b, 2006) indicating the existence of an alternative, non-neurotrophin-dependent TrkB receptor signaling.

Zinc-mediated TrkB transactivation

Transactivation refers to a process whereby a given receptor and its downstream signaling is activated by a stimulus that does not interact directly with the receptor (Carpenter 1999). Prior work demonstrated the transactivation of TrkB in cultured hippocampal neurons by two G protein-coupled receptor ligands, adenosine, pituitary adenylate cyclase-activating peptide (PACAP) and epidermal growth factor receptor (EGFR) (Lee and Chao 2001; Lee et al. 2002; Rajagopal et al. 2004; Puehringer et al. 2013). Transactivation of TrkB has been shown to have biological consequences as it modulates survival of motoneurons after facial nerve lesioning (Wiese et al. 2007) and regulates migration of early neuronal cells to their final position in the developing cortex (Puehringer et al. 2013). Moreover, the divalent cation, zinc has been shown to transactivate TrkB by a neurotrophin-independent and Src- and activity-dependent mechanism resulting in the potentiation of the hippocampal mossy fiber-CA3 pyramidal cell synapse (Huang et al. 2008). The divalent cation zinc is a biologically essential element for brain physiology from early neonatal development to adulthood (Frederickson et al. 2000; Maret and Sandstead 2006). While the majority of zinc in the CNS is permanently bound to zinc-dependent enzymes and other proteins (Berg and Shi 1996) about 10% of it is suggested to be not ligand-associated and to be mostly localized within glutamatergic synaptic vesicles in the hippocampus (Franco-Pons et al. 2000; Takeda 2000) and the cortex (Frederickson and Moncrieff 1994; Frederickson et al. 2000). Here we show that inhibition of Src family kinases as well as scavenging of zinc or depleting zinc by downregulating the zinc transporter ZnT-3 results in impairment in their dendritic complexity and spine density specifically in BDNF-depleted pyramidal neurons. Thus, we suggest the hypothesis that in the absence of BDNF zinc may be able to at least partially compensate the BDNF function by promoting the transactivation of TrkB via the phosphorylation of tyrosine residues Y705/Y706 by the Src family kinases. Interestingly, the hippocampus appears to be the most responsive region to either a deficiency or an excess of zinc (Suh et al. 2009; Takeda and Tamano 2014). Perturbation of zinc homeostasis in hippocampal neurons is also linked to cognitive decline under stress or in pathological conditions (Flinn et al. 2005; Linkous et al. 2009a, b; Takeda and Tamano 2014). In addition, zinc as also BDNF (Castren and Kojima 2017) exhibits antidepressant-like effects in chronic mild stress animal models of depression (Kroczka et al. 2001; Nowak et al. 2003; Rosa et al. 2003) as well as in human depression by the beneficial effect of zinc supplementation in antidepressant therapy (Nowak et al. 2003). While we cannot exclude that other transactivators of TrKB may also play a role in compensating the absence of BDNF for glutamatergic cortical and hippocampal neurons, our results are in agreement with a possible role of zinc in modulating TrkB activation in a BDNF-independent manner and thus contribute at clarifying how a possible functional convergence between zinc and BDNF signaling via the TrkB receptor at synapses can impact nervous system function both in health and disease.

Acknowledgements We are grateful to Diane Mundil, Tania Meßerschmidt and Heike Kessler for their excellent technical assistance and to Martin Rothkegel for experimental advice. This work was supported by the DFG Grant KO 1674/5-1 (to M.K. and M.Z.).

References

Adlard PA, Parncutt JM, Finkelstein DI, Bush AI (2010) Cognitive loss in zinc transporter-3 knock-out mice: a phenocopy for the

synaptic and memory deficits of Alzheimer's disease? J Neurosci 30:1631–1636
Alonso M, Medina JH, Pozzo-Miller L (2004) ERK1/2 activation is necessary for BDNF to increase dendritic spine density in hippocampal CA1 pyramidal neurons. Learn Mem (Cold Spring Harbor, NY) 11:172–178
Baquet ZC, Gorski JA, Jones KR (2004) Early striatal dendrite deficits followed by neuron loss with advanced age in the absence of anterograde cortical brain-derived neurotrophic factor. J Neurosci 24:4250–4258
Bartrup JT, Moorman JM, Newberry NR (1997) BDNF enhances neuronal growth and synaptic activity in hippocampal cell cultures. Neuroreport 8:3791–3794
Berg JM, Shi Y (1996) The galvanization of biology: a growing appreciation for the roles of zinc. Science 271:1081–1085
Bolton MM, Pittman AJ, Lo DC (2000) Brain-derived neurotrophic factor differentially regulates excitatory and inhibitory synaptic transmission in hippocampal cultures. J Neurosci 20:3221–3232
Carpenter G (1999) Employment of the epidermal growth factor receptor in growth factor-independent signaling pathways. J Cell Biol 146:697–702
Castren E, Kojima M (2017) Brain-derived neurotrophic factor in mood disorders and antidepressant treatments. Neurobiol Dis 97:119–126
Castren E, Zafra F, Thoenen H, Lindholm D (1992) Light regulates expression of brain-derived neurotrophic factor mRNA in rat visual cortex. Proc Natl Acad Sci USA 89:9444–9448
Chakravarthy S, Saiepour MH, Bence M, Perry S, Hartman R, Couey JJ, Mansvelder HD, Levelt CN (2006) Postsynaptic TrkB signaling has distinct roles in spine maintenance in adult visual cortex and hippocampus. Proc Natl Acad Sci USA 103:1071–1076
Chan JP, Unger TJ, Byrnes J, Rios M (2006) Examination of behavioral deficits triggered by targeting Bdnf in fetal or postnatal brains of mice. Neuroscience 142:49–58
Chan JP, Cordeira J, Calderon GA, Iyer LK, Rios M (2008) Depletion of central BDNF in mice impedes terminal differentiation of new granule neurons in the adult hippocampus. Mol Cell Neurosci 39:372–383
Chapleau CA, Carlo ME, Larimore JL, Pozzo-Miller L (2008) The actions of BDNF on dendritic spine density and morphology in organotypic slice cultures depend on the presence of serum in culture media. J Neurosci Methods 169:182–190
Choi DW, Koh JY (1998) Zinc and brain injury. Annu Rev Neurosci 21:347–375
Cole TB, Wenzel HJ, Kafer KE, Schwartzkroin PA, Palmiter RD (1999) Elimination od zinc from synaptic vesicles in the intact mouse brain by disruption of the ZnT-3 gene. Proc Natl Acad Sci USA 96:1716–1721
Danzer SC, Pan E, Nef S, Parada LF, McNamara JO (2004) Altered regulation of brain-derived neurotrophic factor protein in hippocampus following slice preparation. Neuroscience 126:859–869
Erickson KI, Prakash RS, Voss MW, Chaddock L, Heo S, McLaren M, Pence BD, Martin SA, Vieira VJ, Woods JA, McAuley E, Kramer AF (2010) Brain-derived neurotrophic factor is associated with age-related decline in hippocampal volume. J Neurosci 30:5368–5375
Flinn JM, Hunter D, Linkous DH, Lanzirotti A, Smith LN, Brightwell J, Jones BF (2005) Enhanced zinc consumption causes memory deficits and increased brain levels of zinc. Physiol Behav 83:793–803
Franco-Pons N, Casanovas-Aguilar C, Arroyo S, Rumia J, Perez-Clausell J, Danscher G (2000) Zinc-rich synaptic boutons in human temporal cortex biopsies. Neuroscience 98:429–435
Frederickson CJ, Danscher G (1990) Zinc-containing neurons in hippocampus and related CNS structures. Prog Brain Res 83:71–84
Frederickson CJ, Moncrieff DW (1994) Zinc-containing neurons. Biol Signals 3:127–139
Frederickson CJ, Suh SW, Silva D, Frederickson CJ, Thompson RB (2000) Importance of zinc in the central nervous system: the zinc-containing neuron. J Nutr 130:1471s–1483s
Frederickson CJ, Suh SW, Koh JY, Cha YK, Thompson RB, LaBuda CJ, Balaji RV, Cuajungco MP (2002) Depletion of intracellular zinc from neurons by use of an extracellular chelator in vivo and in vitro. J Histochem Cytochem 12:1659–1662
Frederickson CJ, Koh JY, Bush AI (2005) The neurobiology of zinc in health and disease. Nat Rev Neurosci 6:449–462
Friedman WJ, Black IB, Kaplan DR (1998) Distribution of the neurotrophins brain-derived neurotrophic factor, neurotrophin-3, and neurotrophin-4/5 in the postnatal rat brain: an immunocytochemical study. Neuroscience 84:101–114
Gao X, Smith GM, Chen J (2009) Impaired dendritic development and synaptic formation of postnatal-born dentate gyrus granular neurons in the absence of brain-derived neurotrophic factor signaling. Exp Neurol 215:178–190
Gorski JA, Zeiler SR, Tamowski S, Jones KR (2003) Brain-derived neurotrophic factor is required for the maintenance of cortical dendrites. J Neurosci 23:6856–6865
He W, Lu Y, Qahwash I, Hu XY, Chang A, Yan R (2004a) Reticulon family members modulate BACE1 activity and amyloid-beta peptide generation. Nat Med 10:959–965
He XP, Kotloski R, Nef S, Luikart BW, Parada LF, McNamara JO (2004b) Conditional deletion of TrkB but not BDNF prevents epileptogenesis in the kindling model. Neuron 43:31–42
He XP, Butler L, Liu X, McNamara JO (2006) The tyrosine receptor kinase B ligand, neurotrophin-4, is not required for either epileptogenesis or tyrosine receptor kinase B activation in the kindling model. Neuroscience 141:515–520
Hong EJ, McCord AE, Greenberg ME (2008) A biological function for the neuronal activity-dependent component of Bdnf transcription in the development of cortical inhibition. Neuron 60:610–624
Horch HW, Kruttgen A, Portbury SD, Katz LC (1999) Destabilization of cortical dendrites and spines by BDNF. Neuron 23:353–364
Huang YZ, McNamara JO (2010) Mutual regulation of Src family kinases and the neurotrophin receptor TrkB. J Biol Chem 285:8207–8217
Huang EJ, Reichardt LF (2001) Neurotrophins: roles in neuronal development and function. Annu Rev Neurosci 24:677–736
Huang YZ, Pan E, Xiong ZQ, McNamara JO (2008) Zinc-mediated transactivation of TrkB potentiates the hippocampal mossy fiber-CA3 pyramid synapse. Neuron 57:546–558
Ip NY, Ibanez CF, Nye SH, McClain J, Jones PF, Gies DR, Belluscio L, Le Beau MM, Espinosa R III, Squinto SP et al (1992) Mammalian neurotrophin-4: structure, chromosomal localization, tissue distribution, and receptor specificity. Proc Natl Acad Sci USA 89:3060–3064
Ivkovic S, Ehrlich ME (1999) Expression of the striatal DARPP-32/ARPP-21 phenotype in GABAergic neurons requires neurotrophins in vivo and in vitro. J Neurosci 19:5409–5419
Jeanneteau F, Chao MV (2006) Promoting neurotrophic effects by GPCR ligands. Novartis Found Symp 276:181–189 **(discussion 189–192, 187–233, 181–275)**
Ji Y, Pang PT, Feng L, Lu B (2005) Cyclic AMP controls BDNF-induced TrkB phosphorylation and dendritic spine formation in mature hippocampal neurons. Nat Neurosci 8:164–172
Ji Y, Lu Y, Yang F, Shen W, Tang TT, Feng L, Duan S, Lu B (2010) Acute and gradual increases in BDNF concentration elicit distinct signaling and functions in neurons. Nat Neurosci 13:302–309
Jones KR, Farinas I, Backus C, Reichardt LF (1994) Targeted disruption of the BDNF gene perturbs brain and sensory neuron development but not motor neuron development. Cell 76:989–999
Kellner Y, Godecke N, Dierkes T, Thieme N, Zagrebelsky M, Korte M (2014) The BDNF effects on dendritic spines of mature hippocampal neurons depend on neuronal activity. Front Synaptic Neurosci 6:5

Kohara K, Kitamura A, Adachi N, Nishida M, Itami C, Nakamura S, Tsumoto T (2003) Inhibitory but not excitatory cortical neurons require presynaptic brain-derived neurotrophic factor for dendritic development, as revealed by chimera cell culture. J Neurosci 23:6123–6131

Kohara K, Yasuda H, Huang Y, Adachi N, Sohya K, Tsumoto T (2007) A local reduction in cortical GABAergic synapses after a loss of endogenous brain-derived neurotrophic factor, as revealed by single-cell gene knock-out method. J Neurosci 27:7234–7244

Korets-Smith E, Lindemann L, Tucker KL, Jiang C, Kabacs N, Belteki G, Haigh J, Gertsenstein M, Nagy A (2004) Cre recombinase specificity defined by the tau locus. Genesis 40:131–138

Kroczka B, Branski P, Palucha A, Pilc A, Nowak G (2001) Antidepressant-like properties of zinc in rodent forced swim test. Brain Res Bull 55:297–300

Kwon HB, Sabatini BL (2011) Glutamate induces de novo growth of functional spines in developing cortex. Nature 474:100–104

Lee FS, Chao MV (2001) Activation of Trk neurotrophin receptors in the absence of neurotrophins. Proc Natl Acad Sci USA 98:3555–3560

Lee FS, Rajagopal R, Kim AH, Chang PC, Chao MV (2002) Activation of Trk neurotrophin receptor signaling by pituitary adenylate cyclase-activating polypeptides. J Biol Chem 277:9096–9102

Linkous DH, Flinn JM, Koh JY, Lanzirotti A, Bertsch PM, Jones BF, Giblin LJ, Frederickson CJ (2008) Evidence that the ZNT3 protein controls the total amount of elemental zinc in synaptic vesicles. J Histochem Cytochem 56(1):3–6

Linkous DH, Adlard PA, Wanschura PB, Conko KM, Flinn JM (2009a) The effects of enhanced zinc on spatial memory and plaque formation in transgenic mice. J Alzheimers Dis 18:565–579

Linkous DH, Flinn JM, Koh JY, Lanzirotti A, Bertsch PM, Jones BF, Giblin LJ, Frederickson CJ (2009b) Evidence that the ZnT-3 protein controls the total amount id elemental zinc in synaptic vesicles. J Histochem Cytochem 56(1):3–6

Maret W, Sandstead HH (2006) Zinc requirements and the risks and benefits of zinc supplementation. J Trace Elem Med Biol Organ Soc Miner Trace Elem (GMS) 20:3–18

Marty S, Berninger B, Carroll P, Thoenen H (1996) GABAergic stimulation regulates the phenotype of hippocampal interneurons through the regulation of brain-derived neurotrophic factor. Neuron 16:565–570

Marty S, Wehrle R, Sotelo C (2000) Neuronal activity and brain-derived neurotrophic factor regulate the density of inhibitory synapses in organotypic slice cultures of postnatal hippocampus. J Neurosci 20:8087–8095

McAllister AK, Lo DC, Katz LC (1995) Neurotrophins regulate dendritic growth in developing visual cortex. Neuron 15:791–803

McAllister AK, Katz LC, Lo DC (1996) Neurotrophin regulation of cortical dendritic growth requires activity. Neuron 17:1057–1064

McAllister AK, Katz LC, Lo DC (1997) Opposing roles for endogenous BDNF and NT-3 in regulating cortical dendritic growth. Neuron 18(5):767–778

McAllister AK, Katz LC, Lo DC (1999) Neurotrophins and synaptic plasticity. Annu Rev Neurosci 22:295–318

Minichiello L (2009) TrkB signalling pathways in LTP and learning. Nat Rev Neurosci 10:850–860

Mizuno K, Carnahan J, Nawa H (1994) Brain-derived neurotrophic factor promotes differentiation of striatal GABAergic neurons. Dev Biol 165:243–256

Monteggia LM, Luikart B, Barrot M, Theobold D, Malkovska I, Nef S, Parada LF, Nestler EJ (2007) Brain-derived neurotrophic factor conditional knockouts show gender differences in depression-related behaviors. Biol Psychiatry 61:187–197

Nowak G, Siwek M, Dudek D, Zieba A, Pilc A (2003) Effect of zinc supplementation on antidepressant therapy in unipolar depression: a preliminary placebo-controlled study. Pol J Pharmacol 55:1143–1147

Puehringer D, Orel N, Luningschror P, Subramanian N, Herrmann T, Chao MV, Sendtner M (2013) EGF transactivation of Trk receptors regulates the migration of newborn cortical neurons. Nat Neurosci 16:407–415

Rajagopal R, Chen ZY, Lee FS, Chao MV (2004) Transactivation of Trk neurotrophin receptors by G-protein-coupled receptor ligands occurs on intracellular membranes. J Neurosci 24:6650–6658

Rauskolb S, Zagrebelsky M, Dreznjak A, Deogracias R, Matsumoto T, Wiese S, Erne B, Sendtner M, Schaeren-Wiemers N, Korte M, Barde YA (2010) Global deprivation of brain-derived neurotrophic factor in the CNS reveals an area-specific requirement for dendritic growth. J Neurosci 30:1739–1749

Rios M, Fan G, Fekete C, Kelly J, Bates B, Kuehn R, Lechan RM, Jaenisch R (2001) Conditional deletion of brain-derived neurotrophic factor in the postnatal brain leads to obesity and hyperactivity. Mol Endocrinol 15:1748–1757

Rosa AO, Lin J, Calixto JB, Santos AR, Rodrigues AL (2003) Involvement of NMDA receptors and L-arginine-nitric oxide pathway in the antidepressant-like effects of zinc in mice. Behav Brain Res 144:87–93

Rutherford LC, DeWan A, Lauer HM, Turrigiano GG (1997) Brain-derived neurotrophic factor mediates the activity-dependent regulation of inhibition in neocortical cultures. J Neurosci 17:4527–4535

Schen H, Zhang Y, Xu J, Long J, Qin H, Liu F, Guo J (2007) Zinc distribution and expression pattern of ZnT-3 in mouse brain. Biol Trace Elem Res 119(2):166–174

Segal RA, Bhattacharyya A, Rua LA, Alberta JA, Stephens RM, Kaplan DR, Stiles CD (1996) Differential utilization of Trk autophosphorylation sites. J Biol Chem 271:20175–20181

Seil FJ, Drake-Baumann R (2000) TrkB receptor ligands promote activity-dependent inhibitory synaptogenesis. J Neurosci 20:5367–5373

Sholl DA (1953) Dendritic organization in the neurons of the visual and motor cortices of the cat. J Anat 87:387–406

Sindreu C, Palmiter RD, Storm DR (2011) Zinc transporter ZnT-3 regulates presynaptic Erk1/2 signaling and hippocampus-dependent memory. Proc Natl Acad Sci USA 108:3366–3370

Stranahan AM (2011) Physiological variability in brain-derived neurotrophic factor expression predicts dendritic spine density in the mouse dentate gyrus. Neurosci Lett 495:60–62

Suh SW, Won SJ, Hamby AM, Yoo BH, Fan Y, Sheline CT, Tamano H, Takeda A, Liu J (2009) Decreased brain zinc availability reduces hippocampal neurogenesis in mice and rats. J cereb Blood Flow Metab Off J Int Soc Cereb Blood Flow Metab 29:1579–1588

Takeda A (2000) Movement of zinc and its functional significance in the brain. Brain Res Brain Res Rev 34:137–148

Takeda A, Tamano H (2014) Cognitive decline due to excess synaptic Zn(2+) signaling in the hippocampus. Front Aging Neurosci 6:26

Tolwani RJ, Buckmaster PS, Varma S, Cosgaya JM, Wu Y, Suri C, Shooter EM (2002) BDNF overexpression increases dendrite complexity in hippocampal dentate gyrus. Neuroscience 114:795–805

Turrigiano G (2007) Homeostatic signaling: the positive side of negative feedback. Curr Opin Neurobiol 17:318–324

Tyler WJ, Pozzo-Miller LD (2001) BDNF enhances quantal neurotransmitter release and increases the number of docked vesicles at the active zones of hippocampal excitatory synapses. J Neurosci 21:4249–4258

Tyler WJ, Pozzo-Miller L (2003) Miniature synaptic transmission and BDNF modulate dendritic spine growth and form in rat CA1 neurones. J Physiol 553:497–509

Unger TJ, Calderon GA, Bradley LC, Sena-Esteves M, Rios M (2007) Selective deletion of Bdnf in the ventromedial and dorsomedial hypothalamus of adult mice results in hyperphagic behavior and obesity. J Neurosci 27:14265–14274

Vicario-Abejon C, Collin C, McKay RD, Segal M (1998) Neurotrophins induce formation of functional excitatory and inhibitory synapses between cultured hippocampal neurons. J Neurosci 18:7256–7271

von Bohlen und Halbach O (2010) Involvement of BDNF in age-dependent alterations in the hippocampus. Front Aging Neurosci. https://doi.org/10.3389/fnagi.2010.00036

Wang L, Chang X, She L, Xu D, Huang W, Poo MM (2015) Autocrine action of BDNF on dendrite development of adult-born hippocampal neurons. J Neurosci 35:8384–8393

Waterhouse EG, An JJ, Orefice LL, Baydyuk M, Liao GY, Zheng K, Lu B, Xu B (2012) BDNF promotes differentiation and maturation of adult-born neurons through GABAergic transmission. J Neurosci 32:14318–14330

Wenzel HJ, Cole TB, Born DE, Schwartzkroin PA, PAlmiter RD (1997) Ultrastructural localization of zinc transporter-3 (ZnT-3) to synaptic vesicle membranes within mossy fibers boutons in the hippocampus of mouse and monkeys. Proc Natl Acad Sci USA 94:12676–12681

Widmer HR, Hefti F (1994) Neurotrophin-4/5 promotes survival and differentiation of rat striatal neurons developing in culture. Eur J Neurosci 6:1669–1679

Wiese S, Jablonka S, Holtmann B, Orel N, Rajagopal R, Chao MV, Sendtner M (2007) Adenosine receptor A2A-R contributes to motoneuron survival by transactivating the tyrosine kinase receptor TrkB. Proc Natl Acad Sci USA 104(43):17210–17215

Yacoubian TA, Lo DC (2000) Truncated and full-length TrkB receptors regulate distinct modes of dendritic growth. Nat Neurosci 3:342–349

Yamada MK, Nakanishi K, Ohba S, Nakamura T, Ikegaya Y, Nishiyama N, Matsuki N (2002) Brain-derived neurotrophic factor promotes the maturation of GABAergic mechanisms in cultured hippocampal neurons. J Neurosci 22:7580–7585

Zagrebelsky M, Korte M (2014) Form follows function: BDNF and its involvement in sculpting the function and structure of synapses. Neuropharmacology 76(Pt C):628–638

Zagrebelsky M, Schweigreiter R, Bandtlow CE, Schwab ME, Korte M (2010) Nogo-A stabilizes the architecture of hippocampal neurons. J Neurosci 30:13220–13234